



## *Eucommia ulmoides* leaf as an alternative substrate for kombucha fermentation: the role of microbial communities in dynamics and metabolic profile

Linfeng Wang<sup>a,b,c,1</sup>, Erfeng Wang<sup>a,b,c,1</sup>, Weipeng Wang<sup>a,b,c</sup>,  
Wei Zhang<sup>a,b,c</sup>, Yifan Ge<sup>a,b,c</sup>, Xiaokang Cao<sup>a,b,c</sup>, Hong (Sabrina) Tian<sup>d</sup>,  
Xingke Li<sup>a,b,c,\*</sup>, Xianfeng Zhu<sup>a,b,c,\*</sup>

<sup>a</sup> School of Life Sciences, Henan University, Kaifeng 475004, China

<sup>b</sup> Henan Key Laboratory of Synthetic Biology and Biomanufacturing, Kaifeng 475004, China

<sup>c</sup> Engineering Research Center for Applied Microbiology of Henan Province, Kaifeng 475004, China

<sup>d</sup> School of Food Technology and Natural Sciences, College of Sciences, Massey University, Palmerston North 4442, New Zealand

### ARTICLE INFO

#### Keywords:

*Eucommia ulmoides* leaf  
Kombucha  
Microbial diversity  
Metabolomics

### ABSTRACT

*Eucommia ulmoides* leaf (EUL) was introduced as a novel fermentation substrate to replace traditional tea in kombucha. High-performance liquid chromatography, untargeted metabolomics, and high-throughput sequencing were applied to understand the potential relationships during fermentation. EUL kombucha exhibited slower sugar consumption rate and superior in vitro antioxidant activity compared with traditional kombucha. Total polyphenols, geniposidic acid, pinoreosin diglucoside, and rutin demonstrated an increasing trend, whereas total flavonoids and chlorogenic acid contents considerably decreased. Metabolite profiling revealed 211 positive and 165 negative ion components in samples fermented for 0, 4, and 8 days. *Komagataeibacter* and *Gluconobacter* were the dominant bacterial genera while *Hanseniaspora*, *Dekkera*, and *Kregervanrija* dominated the yeast community. The dominant microbial genera could have regulated nucleotide metabolism, pentose and glucuronic acid-related conversions, ascorbic acid and aldehyde metabolism, and flavonoid biosynthesis, leading to changes in the expression of differential metabolites of EUL kombucha. The findings support innovation in kombucha development.

### 1. Introduction

Kombucha is a traditional fermented tea beverage, which is made by mixing microorganisms such as acetic acid bacteria (AAB), yeast and lactic acid bacteria with tea sugar and water under natural fermentation conditions (Cardoso et al., 2020; De Filippis et al., 2018). Kombucha is rich in polyphenolic compounds, organic acids, vitamins, amino acids and minerals (Mohd Ariff et al., 2023). Kombucha supports various biological activities, such as liver protection, cancer prevention, digestive support, immunity enhancement, and inhibition of pathogenic bacteria (Esatbeyoglu et al., 2024; Martínez Leal et al., 2018). Owing to its unique taste and potential health benefits, kombucha has gained global popularity in recent decades (Chakravorty et al., 2019; Jakubczyk et al., 2024). The traditional raw material required for fermenting

kombucha is tea leaf, primarily black and green tea. Some studies have used other types of tea leaves, fruit juices, herb infusions, and even by-products of the food industry as alternative substrates for making novel kombucha (Anantachoke et al., 2023; Emiljanowicz & Malinowska-Pańczyk, 2020; Freitas et al., 2022; Xu et al., 2025). Of all the alternative substrates, medicinal and food homologous herbs demonstrated promising effects, as their abundant bioactive compounds can not only modulate fermentation characteristics but also enhance the functional properties of kombucha.

*Eucommia ulmoides* leaf (EUL), a Chinese herbal medicine with the homology of medicine and food, is the dried leaf of *E. ulmoides* Oliv. (Wang et al., 2020; Yuan et al., 2013). *Eucommiae* tea, made from EULs, is commonly marketed in China, Japan, and Korea as a functional health food. *Eucommiae* tea is promoted for various health benefits, such as

\* Corresponding authors at: School of Life Sciences, Henan University, Kaifeng 475004, China.

E-mail addresses: [tianxing1230@henu.edu.cn](mailto:tianxing1230@henu.edu.cn) (X. Li), [zhuxf73@163.com](mailto:zhuxf73@163.com) (X. Zhu).

<sup>1</sup> These authors equally contributed to this study.

weight management, antiosteoporotic effects, diabetes management, and gastrointestinal protection (Duan et al., 2024; Shi et al., 2022; Xu et al., 2018). Modern pharmacological studies suggest that the health benefits of *Eucommia* tea comes from the bioactive components it contains, namely iridoids (such as geniposidic acid (GPA) or aucubin), phenolic acids (e.g., caffeic acid), and flavonoids (including catechins) (Huang et al., 2023; Li, Fu, et al., 2022). In addition to the raw material, the nutrients in kombucha are influenced by the metabolites produced during the fermentation process of the symbiotic microbial community (Li, Wang, et al., 2023; Xu et al., 2024; Zheng et al., 2024).

Precise determination of the microbial composition of kombucha is inherently complex, as it is shaped not only by the tea substrate and the fermentation microbiota but also by fermentation parameters, sugar concentration, and geographic origin, all of which contribute to the remarkable diversity of the microbial community of kombucha (Chen et al., 2022; Mohd Ariff et al., 2023). Various technical methods have been developed to better understand the metabolites and biological pathways involved in the fermentation of kombucha (Tefon-Öztürk et al., 2023). The LC-MS technology offers high sensitivity and specificity, enabling effective separation and identification of metabolites. Furthermore, the technology facilitates a deeper exploration of the products and intermediates involved in the metabolism of kombucha fermentation (Liao et al., 2022; Liu & Locasale, 2017). The emergence of a high-throughput sequencing technology enables a comprehensive understanding of the core microorganisms involved in kombucha fermentation by revealing the dynamics of microbial populations, which regulate the mixed fermentation system and ensure product quality for standardized production (Li, Wang, et al., 2023; Zeng et al., 2022).

Given the limited number of systematic studies on the dynamic changes in microbial communities and metabolites during the fermentation of EUL kombucha, this study employs a multifaceted approach that integrates component content determination, untargeted metabolomics, and ITS/16S rRNA sequencing. By visualizing the major quality components, metabolomic signatures, and microbial features throughout fermentation, we systematically elucidate the evolution of physicochemical properties, the dynamics of active components, and their correlations with microbial community succession. In addition, correlation analysis between the microbiota and crucial metabolites clarifies the potential mechanisms that are driven by microbes involved in the formation of functional components. On the basis of these objectives, the study is expected to provide scientific references for the development of new kombucha beverages exhibiting superior sensory qualities and functional properties.

## 2. Materials and methods

### 2.1. Reagents and chemical standards

EUL was harvested in 2024 in Kaifeng (Henan Province, China). A kombucha starter culture was obtained from a home workshop conducted in Hefei (Anhui Province, China). Black tea was purchased in March 2023 from Wuyishan (Fujian Province, China), and cane sugar was obtained from a local supermarket (Kaifeng, China). Formic acid, methanol, ethanol, and acetonitrile were purchased from McLean Chemical Factory (Shanghai, China). Acetic, malic, succinic, oxalic, citric, chlorogenic acids (CA), pinosresinol diglucoside (PD), GPA, rutin (RU), and gallic acid (purity  $\geq 99\%$ ) were purchased from Beijing Solabio Technology Co., Ltd. (Beijing, China). Glucose, sulfuric acid, sodium hydroxide, sodium carbonate, and phenol were purchased from Sinopharm Chemical Reagents Co., Ltd. (Shanghai, China). 1,1-Diphenyl-2-picrylhydrazyl (DPPH) was purchased from Sangon Biotech Co., Ltd. (Shanghai, China).

### 2.2. Kombucha preparation using EUL

The method used for activating the kombucha starter culture was

adopted from the previously reported protocols, with slight modifications (Healy et al., 2024; Jakubczyk et al., 2020). First, 10 g/L of black tea was boiled for 10 min and filtered through a cheesecloth to remove the tea leaves. Subsequently, 100 g/L of sucrose was added and dissolved in the tea broth. Thereafter, 10% (v/v) of the kombucha starter culture was inoculated and the mixture was incubated at 30 °C for 8 days. The activated culture was used for EUL kombucha fermentation.

Following the method of Xiong et al. (2023), this study utilized EUL as a raw material and retained the tea residues during fermentation to prepare kombucha beverages. Precisely, 2.0 g of dried EUL and 18.0 g of sucrose were mixed with 180 mL of deionized water and sterilized at 115 °C for 20 min. After cooling down the mixture to 25 °C, it was inoculated with 10% (v/v) of activated kombucha inoculum in a laminar flow hood. The prepared mixture was allowed to ferment at 30 °C for 8 days. Samples were aseptically collected on days 0, 2, 4, 6, and 8 for subsequent analysis. The preparation process of EUL kombucha is shown in Fig. S1.

### 2.3. Determination of physical and chemical compositions

#### 2.3.1. Determination of pH, total acid, and organic acid contents

The pH of the EUL kombucha samples was measured using a pH meter. The total acid content, determined via acid–base titration with NaOH, was expressed as acetic acid equivalents (Dartora et al., 2023; Li, Bi, et al., 2022). The calculation method for total acid is shown in Eq. (1) as follows:

$$\text{Total acid (g/L)} = [c \times (V_1 - V_2) \times k \times F] / m \times 1000, \quad (1)$$

where  $c$  is the concentration of the NaOH titrant,  $V_1$  and  $V_2$  are the titrant volumes of the sample and blank, respectively,  $k$  is the acid-specific molar mass conversion factor,  $F$  is the dilution factor,  $m$  is the sample mass, and 1000 is the conversion factor.

The organic acid content was determined using the method described by Zhang et al. (2020). A CarboMix H-NP5 column (300 × 7.8 mm, 5 μm) was used. The mobile phase comprised a 2.5-mmol/L sulfuric acid aqueous solution, and isocratic elution was performed at a flow rate of 0.6 mL/min. Column temperature, injection volume, and detection wavelength were set at 55 °C, 10 μL, and 210 nm, respectively. Standard samples of oxalic, citric, malic, succinic, and acetic acids were accurately weighed and dissolved in ultrapure water to prepare standard solutions. Linear regression was performed on the peak areas ( $y$ ) of each organic acid and their corresponding concentrations ( $x$ , g/L) to establish a standard curve equation.

#### 2.3.2. Determination of total sugar and total reducing sugar contents

The total sugar content was determined using the phenol–sulfuric acid method, with slight modifications (Özyurt, 2020). A standard curve was generated taking glucose as the standard substance (0.1–0.5 g/L) ( $y = 6.644x + 0.276$ ,  $R^2 = 0.999$ ). Notably, 0.5 mL of the 200-fold diluted supernatant sequentially reacted with 0.5 mL of 6% phenol and 1.5 mL of concentrated sulfuric acid. After thorough mixing and a 10-min reaction, the absorbance was measured at 490 nm.

The total reducing sugar content was determined using the 3,5-dinitrosalicylic acid (DNS) method according to Applegate et al. (2019) with slight modifications. A standard curve was established using glucose solutions at concentrations ranging from 0.1 to 0.9 g/L ( $y = 0.878x + 0.022$ ,  $R^2 = 0.998$ ). A 0.5-mL aliquot of the 200-fold diluted supernatant was mixed with 0.5 mL of DNS solution and heated in a boiling water bath for 5 min. Following cooling, the mixture was diluted with 4 mL of deionized water, followed by the measurement of absorbance at 540 nm.

### 2.4. Determination of bioactive compounds content

#### 2.4.1. Determination of flavonoid and total phenolic contents

The total polyphenol content was determined using a modified

Folin–Ciocalteu method. A standard curve ( $y = 6.107x + 0.092$ ,  $R^2 = 0.997$ ) was established using gallic acid (0.01–0.1 g/L) (Li, Chen, et al., 2023). A 0.5-mL aliquot of the 200-fold diluted supernatant was mixed with 2.5 mL of 10% phenol solution, vortexed for 5 min, and followed by the addition of 2 mL of 7.5% sodium carbonate solution. After 60 min of incubation in the dark, the absorbance was measured at 765 nm.

The total flavonoid content was determined using the aluminum nitrate–sodium nitrite colorimetric method, with slight modifications (Procházková et al., 2011). A standard curve ( $y = 1.275x + 0.038$ ,  $R^2 = 0.991$ ) was established using RU as the standard substance (0.1–1 g/L). Thereafter, 1 mL of the supernatant was mixed with 0.75 mL of 5% sodium nitrite solution. After the mixture was allowed to stand for 6 min, 0.75 mL of 10% aluminum nitrate solution was added, followed by another 6-min incubation period. Subsequently, 4 mL of 4% sodium hydroxide solution was added, followed by 15 min of incubation. The absorbance was ultimately measured at 510 nm.

#### 2.4.2. Determination of CA, GPA, PD and AU contents

The content of bioactive compounds was determined via high-performance liquid chromatography (HPLC) (Ding et al., 2014) using a Welch Boltimate C18 column (100 × 4.6 mm, 2.7 μm) and a mobile phase comprising acetonitrile (A) and 0.1% formic acid aqueous solution (B) for gradient elution. The specific gradient parameters were set as follows: 0–12 min, 5%–8% (A); 12–20 min, 8%–15% (A); 20–30 min, 15%–20% (A); 30–40 min, 20%–30% (A); 40–45 min, 30%–5% (A); and 45–47 min, 5%–5% (A). The flow rate of the mobile phase was 1 mL/min, the column temperature was 25 °C, the sample injection volume was 10 μL, and the detection wavelength was 238 nm. The content of active components in EUL at different fermentation days was calculated on the basis of the standard curve (μg/mL).

#### 2.5. Determination of antioxidant activity capacity

DPPH radical scavenging activity was determined according to the method described by Thaipong et al. (2006), with some modifications. Notably, 1 mL of the 30-fold diluted sample solution was mixed with 1 mL of 0.1-mmol/L DPPH–ethanol solution. The mixture was thoroughly vortexed and incubated in the dark for 20 min, following which the absorbance at 517 nm was measured and denoted as  $A_1$ . Distilled water mixed with the DPPH–ethanol solution was used as the blank control group, denoted as  $A_0$ . The calculation method for DPPH scavenging rate is shown in Eq. (2).

$$\text{DPPH free radical scavenging rate(\%)} = (A_0 - A_1)/A_0 \times 100 \quad (2)$$

Hydroxyl radical scavenging capacity was determined using the method described by Yang et al. (2022) with slight modifications. Briefly, 1 mL of the supernatant was sequentially mixed with 1 mL of a 9-mmol/L  $\text{FeSO}_4$  and 1 mL of 9-mmol/L salicylic acid–ethanol solution. Following mixing, 1 mL of an 8.8-mmol/L  $\text{H}_2\text{O}_2$  solution was added to initiate the reaction and the mixture was incubated at 37 °C for 30 min. The absorbance was measured at 510 nm. The calculation method for •OH scavenging rate is shown in Eq. (3).

$$\bullet\text{OH free radical scavenging rate(\%)} = [A_0 - (A_m - A_n)]/A_0 \times 100 \quad (3)$$

Total reducing power was determined using the method described by Kłopotek et al. (2005) with slight modifications. First, 0.4 mL of the 10-fold diluted sample (in a 0.2-mol/L phosphate buffer at pH 6.6) was mixed with 0.4 mL of 1% potassium ferricyanide. The mixture was incubated at 50 °C for 0.5 h. Following incubation, 0.4 mL of 10% trichloroacetic acid was added and the resulting mixture was centrifuged at 4000 rpm for 10 min. Subsequently, 0.4 mL of the resulting supernatant was combined with 1.6 mL of distilled water and 80 μL of 0.1% ferric chloride solution. After standing for 10 min, the absorbance was measured at 700 nm against a distilled water blank.

#### 2.6. Untargeted metabolomics analysis

Briefly, 100 μL of the liquid was transferred to a 1.5-mL centrifuge tube. Subsequently, 400 μL of an extraction solution (acetonitrile: methanol = 1:1, v/v) containing 0.02 mg/mL of the internal standard (L-2-chlorophenylalanine) was added. The mixture was homogenized by vortexing it for 30 s, followed by a 30 min of low-temperature ultrasonic extraction at 5 °C and 40 kHz. Following incubation at –20 °C for 30 min, the sample was centrifuged at 13,000g and 4 °C for 15 min. The collected supernatant was dried under nitrogen, reconstituted in 100 μL of acetonitrile/water (1:1, v/v), and vortexed. After low-temperature ultrasonication (5 °C, 40 kHz, 5 min) and a final centrifugation (13,000g, 4 °C, 10 min), the extract was transferred into an autosampler vial for analysis.

The LC–MS/MS analysis of the samples from different fermentation days was performed using an ultra-high performance liquid chromatography tandem Fourier transform mass spectrometry UHPLC–Q Exactive HF-X system (Thermo Fisher, USA). HSS T3 column was used as a chromatographic column (100 × 2.1 mm i.d., 1.8 μm), mobile phase A comprised 95% water +5% acetonitrile (containing 0.1% formic acid), and mobile phase B exhibited 47.5% acetonitrile +47.5% isopropanol +5% water (containing 0.1% formic acid). The sample was separated using the chromatographic column and analyzed via mass spectrometry. Mass scanning range of 70–1050  $m/z$ , sheath gas flow rate of 50 psi, auxiliary gas flow rate of 13 psi, auxiliary gas heating temperature of 425 °C, ion spray voltages were set at +3500 and –3500 V in positive and negative modes, respectively, ion transfer tube temperature was 325 °C, and normalized collision energy was 20–40–60-V cyclic collision energy. The mass spectrometer was operated at resolutions of 60,000 (MS1) and 7500 (MS2) in data-dependent acquisition mode.

#### 2.7. Sequencing of microbial diversity

The EUL kombucha fermentation liquid was prepared according to the method described in Section 2.2. Bacterial cellulose membranes and fermentation liquid were collected from the fermenter on days 0, 4, and 8 and were labeled as D0, D4, and D8, respectively. All the samples were processed in triplicate and stored at –80 °C until analysis. Total DNA was extracted from the microbial communities in samples according to the instructions provided in the DNA extraction kit. The quality of DNA extraction was detected via 1% agarose gel electrophoresis, and DNA concentration and purity were determined using NanoDrop2000 (Thermo Scientific, USA). For amplification of the yeast ITS region and bacterial 16S rRNA gene (V3–V4 region), the primer pairs ITS1F/ITS2R and 338F/806R were used, respectively. The microbial sequencing in these samples was commissioned to Shanghai Majorbio Bio-Pharm Technology Co., Ltd. ([www.majorbio.com](http://www.majorbio.com)).

#### 2.8. Data analysis

Data were expressed as the mean ± standard deviation ( $n = 3$ ) and plotted using Origin 2021 (OriginPro Lab Corp., Northampton, MA, USA). Significance analyses were performed using SPSS 27.0 (IBM SPSS, USA).  $t$ -tests were performed on independent samples for distinguishing the mean values. Here,  $p < 0.05$  was considered significant. The processing and analysis of untargeted metabolomics and bioinformatics data were conducted utilizing the proprietary cloud platform (<https://www.majorbio.com/tools>) of Shanghai Majorbio Bio-Pharm Technology Co., Ltd. Spearman's algorithm was used to plot heat maps of core microbial genera and physicochemical components, bioactive compounds, and various metabolites.

### 3. Results and discussion

#### 3.1. Comparison between traditional kombucha and EUL kombucha

The pH (Fig. 1A) and sugar contents (Fig. 1B and C) were the crucial indicators for evaluating the fermentation process of kombucha. The trends in pH, total sugar, and total reducing sugar contents in the EUL kombucha were comparable to those observed in TK. During the fermentation of EUL kombucha, the pH dropped quickly within the first 2 days, decreasing from  $5.340 \pm 0.028$  to  $2.980 \pm 0.015$  for the EUL group and from  $5.250 \pm 0.028$  to  $2.850 \pm 0.026$  for the TK (black tea) group. At the end of fermentation (D8), the total sugar consumption rate for EUL kombucha was 22.331%, compared with 36.340% for TK. Relative to the initial fermentation stage (D0), the total reducing sugar content in TK was  $78.398 \pm 6.720$  g/L, while that in EUL kombucha was  $40.179 \pm 1.446$  g/L. Pearson correlation analysis showed a strong negative correlation between total sugars and reducing sugars in both EUL kombucha ( $r = -0.975$ ) and TK ( $r = -0.971$ ). Compared with TK, EUL kombucha exhibited a smaller change in sugar content, making it more suitable for individuals who were concerned about blood sugar stability (Liu et al., 2024). The presence of microorganisms in the fermentation broth led to the breakdown of sucrose into glucose and fructose, increasing the total reducing sugar levels and decreasing the total sugar levels. These changes were consistent with the previous research findings (Keshk & Sameshima, 2005; Tu et al., 2024; Watawana et al., 2015).

In vitro antioxidant activity is one of the important indicators for evaluating the functional activity of EUL kombucha. As shown in Fig. 1D–F, the EUL kombucha and TK demonstrated the same trends about antioxidant activity during fermentation, although the antioxidant activity of EUL kombucha was stronger than that of TK. The stronger antioxidant capacity observed in vitro provided a basis for hypothesizing a higher potential to reduce oxidative stress in vivo. The

DPPH radical scavenging rate, the hydroxyl radical scavenging rate, and the reducing power of EUL kombucha were as high as  $80.108\% \pm 1.466\%$ ,  $81.669\% \pm 0.700\%$ , and  $0.352 \pm 0.010$  (OD<sub>700</sub>), accounting for an increase of 11.842%, 50.021%, and 11.430% from the D0, respectively. The differences in antioxidant activity among kombucha fermentation products were primarily attributed to the leaching of flavonoids during fermentation and the synergistic effects of newly formed polyphenolic compounds (Wang et al., 2022). EULs are rich in natural antioxidant components such as CA, PD, and GPA. The microorganisms in kombucha could break down EUL to release more free-form antioxidant components (Jayabalan et al., 2014; Liu et al., 2024; Muhiaddin et al., 2019). Given the small difference between days 4 and 8 and the previously presented results indicating higher values on day 8, fermentation up to the eighth day was considered beneficial from a bioactive standpoint. The results demonstrated that EULs could not only replace black tea in kombucha fermentation but also impart additional beneficial effects.

#### 3.2. Analysis of organic acid in EUL kombucha

Organic acids are a crucial parameter that affects the flavor of kombucha fermentation. As shown in Fig. 2A, the total acid content in EUL kombucha increased throughout fermentation, increasing from an initial  $1.248 \pm 0.004$  to  $38.490 \pm 0.049$  g/L on day 8, reflecting continuous microbial production and acid accumulation (Hur et al., 2014). HPLC analysis revealed (Fig. 2B–F) that acetic acid was the dominant organic acid formed, consistent with the findings of Jayabalan et al. (2010). The dominance could be attributed to yeast and AAB that decomposed glucose and fructose into ethanol or acetic acid (Grassi et al., 2022). Yeast metabolites created a favorable environment for AAB by not only promoting their proliferation but also by providing a vinegar-like flavor to EUL kombucha (Keshk & Sameshima, 2005; Leali et al., 2022; Zubaidah et al., 2017). Malic and oxalic acid contents in

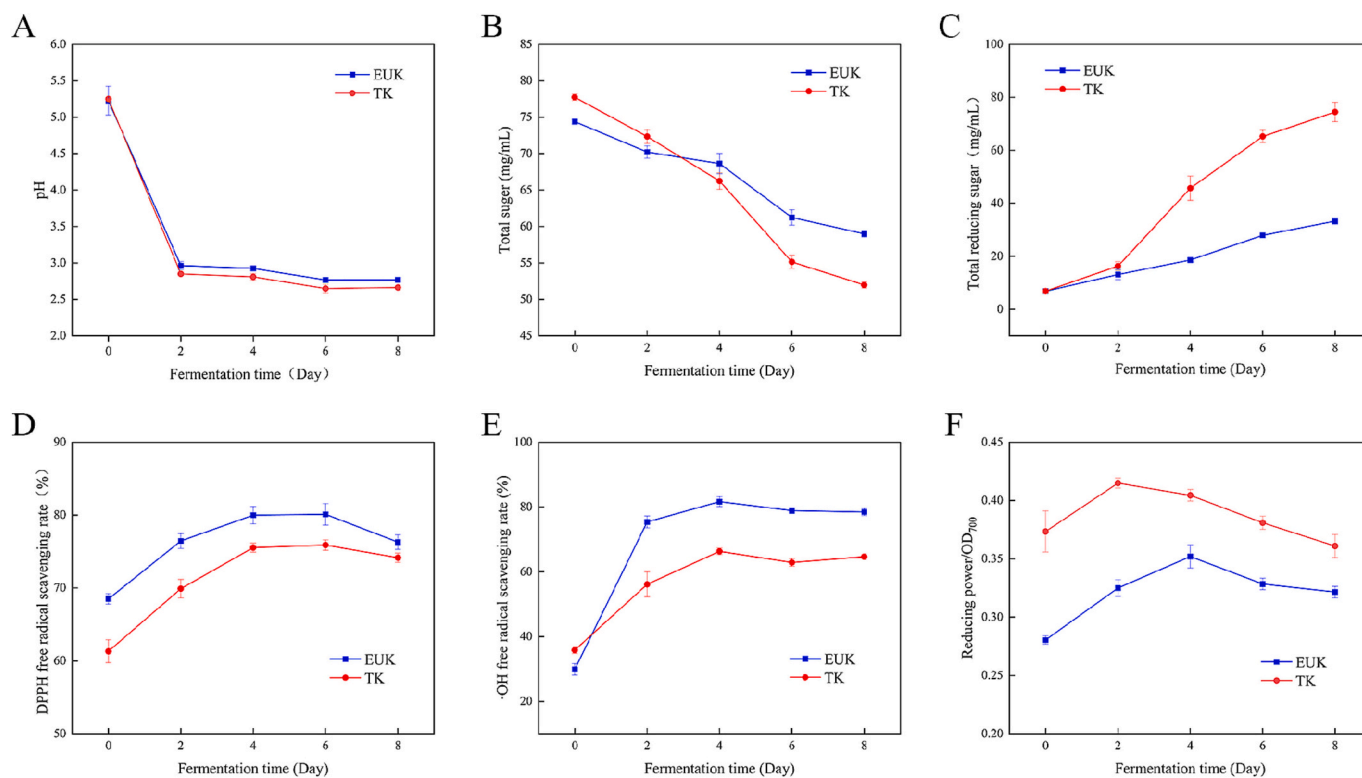


**Fig. 1.** Comparison between traditional kombucha and EUL kombucha at different fermentation times. (A) pH, (B) total sugar content, (C) total reducing sugar content, (D) DPPH radical scavenging activity, (E) hydroxyl radical scavenging activity, and (F) reducing power. EUK: *Eucommia ulmoides* leaf kombucha; TK: traditional (black tea) kombucha. Results are based on colorimetric methods and represent estimates.

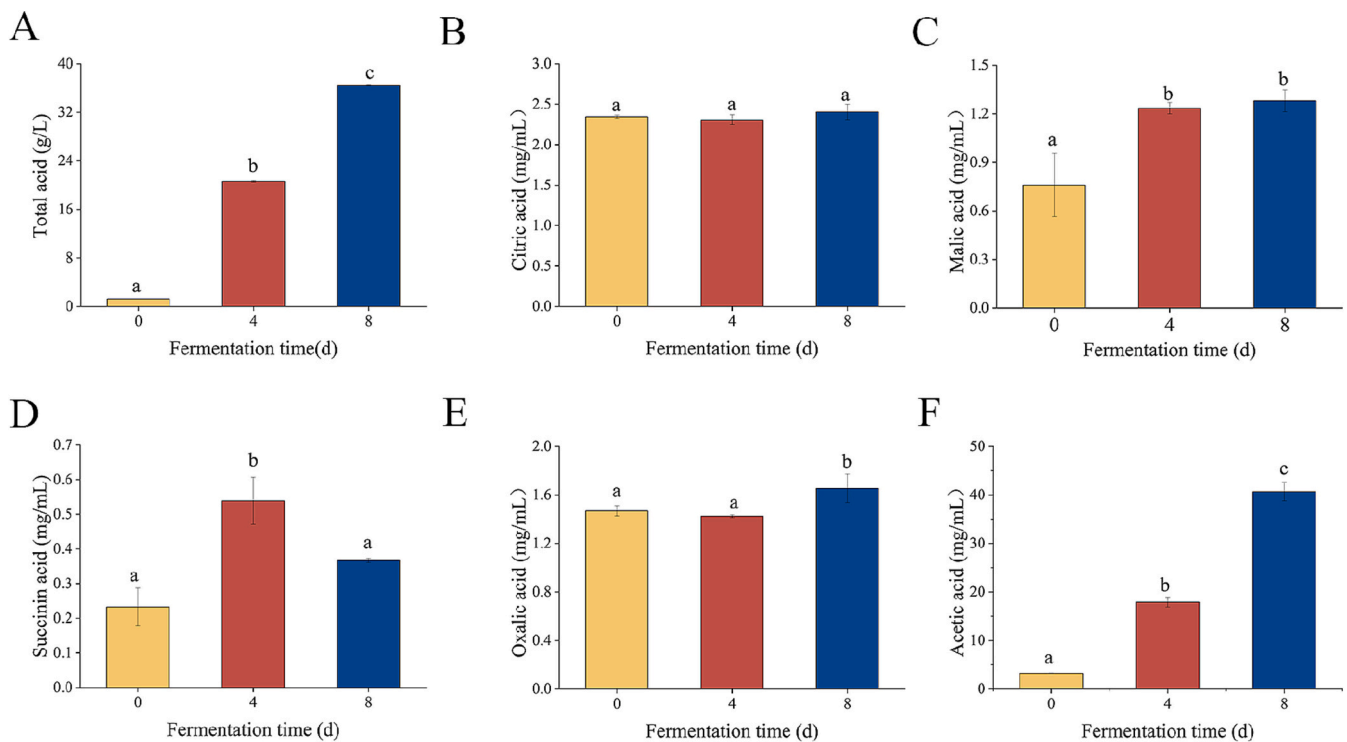


**Fig. 2.** Changes in organic acid content in EUL kombucha at different fermentation times (D0, D4, and D8). (A) total acid, (B) citric acid, (C) malic acid, (D) succinic acid, (E) oxalic acid, and (F) acetic acid contents. Values are expressed as mean  $\pm$  SD ( $n = 3$ ). Means with different letters in the same row differ significantly ( $p < 0.05$ ).

EUL kombucha slightly increased during fermentation, whereas succinic acid content decreased in the later stages of fermentation. Malic acid could be produced by yeasts and aided in liver detoxification while contributing a metallic and green apple-like flavor (Selvaraj & Gurusurthy, 2024; Xu et al., 2022). Oxalic acid exhibited a minimal impact on flavor but required consistent monitoring owing to the potential health risks associated with its high concentration (Ford & Choi, 2013). The sour, salty, and bitter taste imparted by succinic acid was influenced in EUL kombucha, as it was broken down by microorganisms in the later stages into compounds such as succinate, malic acid, and oxaloacetic acid or utilized in amino acid synthesis (Ferreira & Mendes-Faia, 2020; Kitwetcharoen et al., 2023; Mao et al., 2023). By contrast, citric acid, which imparted a fresh and pleasant citrus flavor (Lambros et al., 2022), maintained stable levels with no statistically significant differences observed between days 0, 4, and 8. The stability of citric acid could be owing to the microbial communities within the kombucha system (primarily yeasts and AAB), obtaining a dynamic equilibrium in the production and consumption rates of citric acid (Coton et al., 2017).

### 3.3. Analysis of bioactive components in EUL kombucha

To evaluate the functional properties of the fermented product, the dynamic changes in polyphenols, flavonoids, PD, GPA, RU, and CA in EUL kombucha were quantified. As detailed in Table 1, the total polyphenol content increased continuously with fermentation time, whereas the total flavonoid content showed a progressive decrease. The increase in total polyphenol content was likely attributed to the hydrolysis of bound phenolic compounds via cellulases released by microorganisms (Jayabalan et al., 2017), whereas the decrease in total flavonoid content could be attributed to the structural instability of flavonoids and microbial conversion into glycosides (Cheng et al., 2013; Sun et al., 2015). Compared with previously reported kombucha, the total polyphenol content in EUL kombucha was lower during fermentation, whereas the total flavonoid content was higher (Zheng et al., 2024). This difference

**Table 1**

Changes in the content of active components in the EUL kombucha at different fermentation times.

Compounds( $\mu\text{g/mL}$ )	Fermentation time(d)		
	0	4	8
Total polyphenols	404.860 $\pm$ 0.001 <sup>c</sup>	618.770 $\pm$ 0.021 <sup>b</sup>	671.792 $\pm$ 0.004 <sup>a</sup>
Total flavonoids	534.043 $\pm$ 0.025 <sup>a</sup>	347.720 $\pm$ 0.236 <sup>b</sup>	303.271 $\pm$ 0.008 <sup>c</sup>
Pinoresinol diglucoside	104.012 $\pm$ 3.021 <sup>b</sup>	115.523 $\pm$ 6.184 <sup>a</sup>	124.343 $\pm$ 3.671 <sup>a</sup>
Geniposidic acid	173.641 $\pm$ 5.024 <sup>b</sup>	186.602 $\pm$ 4.554 <sup>ab</sup>	206.931 $\pm$ 13.623 <sup>a</sup>
Rutin	33.905 $\pm$ 0.981 <sup>b</sup>	38.316 $\pm$ 1.052 <sup>a</sup>	38.185 $\pm$ 1.895 <sup>a</sup>
Chlorogenic acid	240.206 $\pm$ 2.893 <sup>a</sup>	230.380 $\pm$ 7.492 <sup>ab</sup>	221.670 $\pm$ 0.951 <sup>b</sup>

Note: Different lowercase letters in the superscripts of the same line (<sup>a</sup>, <sup>b</sup>, and <sup>c</sup>) indicate significant differences in the bioactive compounds in the one-way ANOVA ( $P < 0.05$ ). Values are the mean of three determinations  $\pm$  SD (standard deviation).

could likely be attributed to the distinct fermentation substrates used.

PD and RU increased after 4 days of fermentation (compared with day 0), but there was no notable difference between days 4 and 8, indicating that the increase occurred primarily in the early fermentation phase. GPA and CA markedly changed only after 8 days relative to day 0: GPA increased, whereas CA decreased. However, for both the compounds, there was no difference between days 0 and 4, indicating that the later fermentation stages were the most influential for their variation. The highest values of GPA, PD, and RU increased by 19.17%, 19.55%, and 12.45%, respectively, compared with their initial values. The increased levels of GPA could contribute to its enhanced effects on blood pressure (Liu et al., 2024). CA, a key quality evaluation standard for EUL medicinal materials, decreased by 7.72% from its initial level.

This phenomenon could be attributed to the enzymatic activity of microorganisms, such as  $\beta$ -glucosidase and esterases, which facilitated the transformation of CA (Xiao et al., 2021; Xu et al., 2025). The increase in the content of the three bioactive compounds could be owing to the microorganisms in EUL kombucha that secreted relevant enzymes to hydrolyze sugar glycoside precursors in EUL, facilitating the bioconversion of bioactive compounds such as GPA and PD. The peak concentrations of the three key bioactive components coincided with the period of highest microbial metabolic activity and enzymatic efficiency during the mid-fermentation stage. Compared with TK (Júnior et al., 2022), EUL kombucha developed a distinct bioactive profile during fermentation, which was dominated by unique constituents such as PD, RU, GPA, and CA.

### 3.4. Untargeted metabolomics analysis of EUL kombucha

To comprehensively understand the metabolite composition and structural characteristics throughout the fermentation of EUL kombucha, raw data from the samples collected at different fermentation stages were preprocessed under both positive and negative ionization modes. Notably, 502 compounds were putatively identified in positive ion mode and 356 compounds in negative ion mode. Of these, the number of metabolites annotated to the KEGG database was 211 for the positive ion group and 165 for the negative ion group. The annotated metabolites included 52 types of lipids and lipid molecules; 48 types of organic acids and their derivatives; 82 types of oxygen-containing organic compounds; 49 types of organic heterocyclic compounds; 56 types of benzene, propane, and polyketone compounds; 44 types of benzene ring hydrocarbon compounds; 11 types of nucleic acids/nucleotides and their analogs; seven types of nitrogen-containing organic compounds; 2 sulfur-containing organic compounds; 3 hydrocarbon compounds; 6 alkaloids and their derivatives; 2 lignan compounds; and 14 other types of compounds. PCA revealed (Fig. 3A) that replicate samples from each

fermentation time point closely clustered together within the 95% confidence interval, demonstrating high reproducibility and reliability of the data. PLS-DA was used to more clearly highlight the differences between groups (Fig. 3B). The three sample groups showed clear separation within the 95% confidence interval, demonstrating that fermentation time considerably affected the metabolite composition. The reliability of the model was assessed by conducting the PLS-DA model replacement test (Fig. 3C). The  $Q^2$  regression line on the Y-axis was  $<0.05$ , and both  $R^2$  and  $Q^2$  values were  $\sim 1$ , indicating the robustness and reliability of the model without overfitting.

Fig. 3D–F and Tables S1–3 present 259 markedly different metabolites that are screened and putatively identified between the D4/D0 groups, including 212 upregulated and 57 downregulated metabolites. Two hundred sixty-three considerably different metabolites were screened and putatively identified between the D8/D0 groups, namely 204 upregulated and 59 downregulated metabolites. Between the D8/D4 group, 153 notably different metabolites were screened and putatively identified, including 78 upregulated and 75 downregulated. Volcano plot results indicated that the metabolites in EUL kombucha continuously changed as the fermentation progressed.

During fermentation, the metabolite profile became increasingly complex, with more differential metabolites being produced over time. To elucidate the classification and potential biological roles of such compounds, a comparative analysis was conducted against the KEGG database. Annotating the KEGG metabolic pathways revealed the following results (Table S4–6). Compared with D0, 128 differentially expressed metabolites were screened on the fermentation day four (D4) using a  $p < 0.05$  standard; of them, 104 were notably upregulated and 24 were considerably downregulated. Compared with fermentation D4, 73 differentially expressed metabolites were screened on the fermentation day 8 (D8), of which 39 were considerably upregulated and 34 were markedly downregulated. Compared with D0, 129 differentially expressed metabolites were screened on the fermentation D8, of which

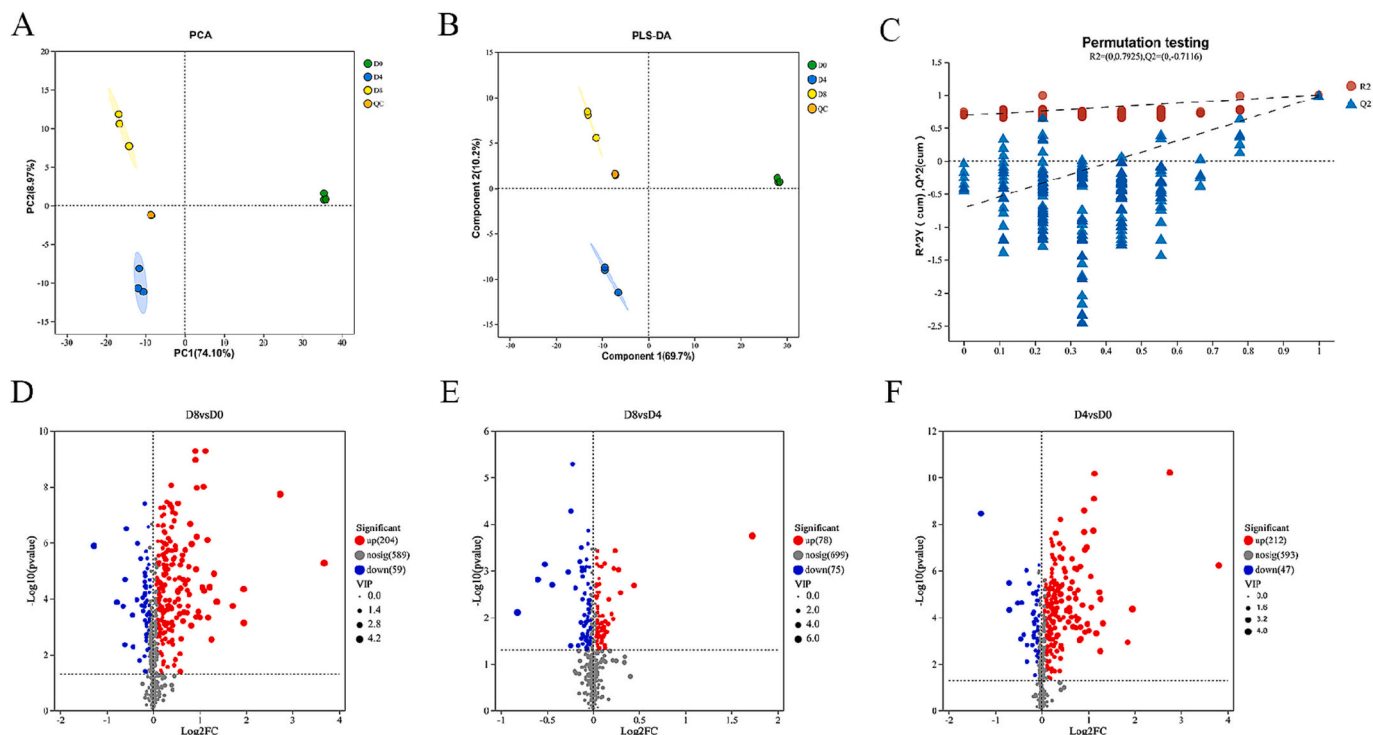


**Fig. 3.** Multivariate statistical analysis of untargeted metabolomics of EUL kombucha at different fermentation times. (A) Principal Component Analysis (PCA) of metabolites. (B) Partial Least Squares–Discriminant Analysis (PLS–DA) model. (C) Validation of the PLS–DA model. (D–F) Volcano plots combining  $t$ -tests, OPLS–DA, and FC screening of differential metabolites, with criteria of  $VIP > 1$  and  $p < 0.05$ . For compounds showing marked differences, refer Supplementary Table S1–3. Each point represents a metabolite: gray indicates nonsignificant differences, blue indicates markedly downregulated metabolites, and red indicates considerably upregulated metabolites. (For interpretation of the references to colour in this figure legend, the reader is referred to the web version of this article.)

96 were markedly upregulated and 33 were considerably downregulated.

KEGG pathway enrichment analysis of differentially abundant metabolites putatively identified the specific pathways they were involved in, thereby elucidating their biological functions. Fig. 4A and B illustrates the KEGG metabolic pathway enrichment analysis and the KEGG pathway differential abundance score of significantly enriched metabolites ( $p < 0.05$ ) in different fermentation day comparison groups. Twenty-nine pathways were screened from the D4/D0 group, among which 18 pathways showed an upward trend and seven pathways showed a downward trend. Of these, the most considerably upregulated pathways with differential metabolite expression trends included the metabolism of acetaldehyde and dicarboxylic acids, the biosynthesis of

valine, leucine, and isoleucine; galactose metabolism; the interconversion of pentoses and glucuronic acid; and the metabolism of ascorbic acid and aldehydes. The pathway with the most markedly downregulated differential metabolite expression trends was the biosynthesis of arginine. In the D8/D4 group, 10 pathways were considerably altered, with six showing upregulation and four showing downregulation. Of these, the metabolic pathways annotated with differential metabolites in the fatty acid biosynthesis and glycosylphosphatidylinositol anchor biosynthesis pathways markedly upregulated, whereas the caffeic acid metabolism pathway considerably downregulated. In the D8/D0 group, 23 metabolic pathways were putatively identified, with 16 showing upregulation and five downregulation. Of these, the metabolic pathways annotated with notably upregulated differential metabolites included

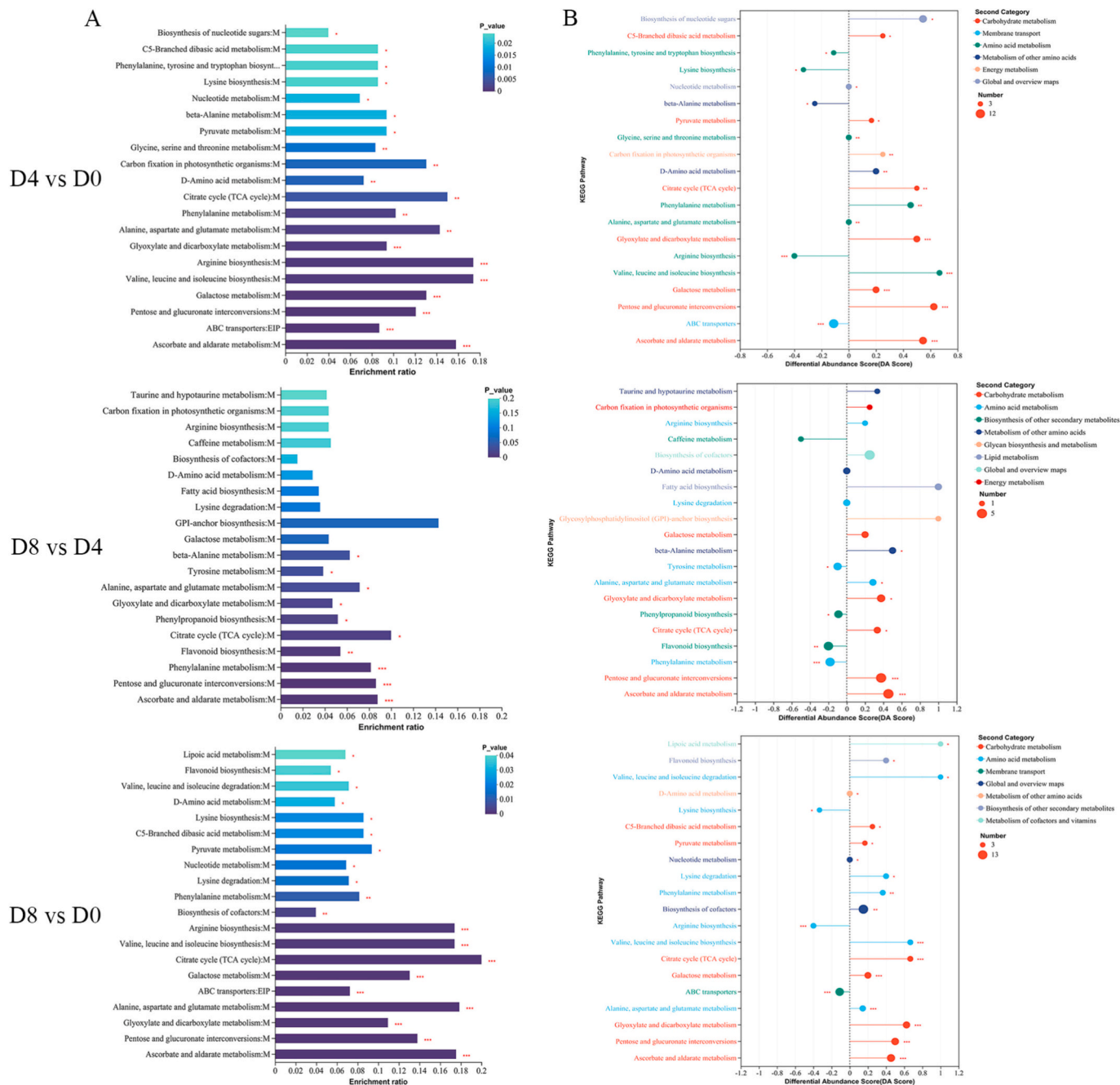


Fig. 4. KEGG metabolic pathway enrichment analysis of EUL kombucha at different fermentation times. (A) KEGG pathway enrichment analysis. (B) KEGG pathway differential abundance scores. The colour gradient of the columns indicates the significance of enrichment, with darker colors denoting greater enrichment of the KEGG term.  $***p < 0.001$ ,  $**p < 0.01$ , and  $*p < 0.05$ .

thioctic acid metabolism; valine, leucine, and isoleucine degradation; valine, leucine, and isoleucine biosynthesis; the citric acid cycle; glycolate and dicarboxylic acid metabolism; and the interconversion of pentose and glucuronic acid, whereas the biosynthesis of lysine considerably downregulated. As fermentation progressed, most metabolic pathways considerably changed and the changes were primarily concentrated in the related amino acid and sugar metabolic pathways.

To elucidate the functional effects and temporal dynamics of differentially expressed metabolites, this study employed variable importance (VIP) analysis to conduct an in-depth analysis of the differentially expressed metabolites that matched with KEGG pathway enrichment analysis. Table S7 presents the representative differentially expressed metabolites screened from the D4/D0 group, which are associated with 33 metabolic pathways. Of these, 55 metabolites showed upregulation, such as glucose lactone, ascorbic acid, and 3-hydroxypyruvic acid, and 16 metabolites showed downregulation, such as sucrose, stachydrine, and aspartic acid. Table S8 presents the representative differentially expressed metabolites screened from the D8/D4 group, which are associated with 23 metabolic pathways. Of these, there were 23 upregulated differentially expressed metabolites, such as glucuronic acid, citric acid, and pyridoxine, and 13 downregulated differentially expressed metabolites, such as *N*-acetylceramide, epigallocatechin, and trans-cinnamic acid. Table S9 lists the representative differentially expressed metabolites screened from the D8/D0 group, which are associated with 38 metabolic pathways. Of these, there were 58 upregulated differentially expressed metabolites, such as sorbitol, succinic acid, and malic acid, and 18 downregulated differentially expressed metabolites, such as adenosine, fructose, and gentianin.

As a key pathway for microbial growth, sugar metabolism was found to produce 31 different carbohydrates after 8 days of fermentation. As the primary carbon source, sucrose continued to decrease, with its VIP value increasing from 1.466 on day 4 to 1.512 on day 8, indicating continuous sucrose consumption by microbes. Concurrently, the expression levels of sugar compounds such as *D*-xylose, *D*-rhamnose, *D*-sorbitol, and *D*-heptose increased. In TK fermentation, yeasts first hydrolyzed sucrose into glucose and fructose (Villarreal-Soto et al., 2019), which were later co-metabolized by yeasts and AAB into primary metabolites, such as ethanol, acetic acid, glucuronic acid, and gluconic acid lactone (May et al., 2019). AAB further metabolized such compounds through pathways such as the tricarboxylic acid cycle and pentose phosphate pathway, producing additional organic acids such as citric, succinic, and  $\alpha$ -ketoglutaric acids (Jayabalan et al., 2007).

As presented in Table S7 and S8, characteristic metabolites, such as gluconic, succinic, and citric acids, generally increased by days 4 and 8 of fermentation, with higher VIP values observed on day 8. Notably, following EUL fermentation, several structurally or metabolically related compounds, namely glucose, citric acid, and succinic acid, were putatively identified and showed increased levels, while the typical markers, such as glucose and acetic acid, were not detected as differentially expressed metabolites. This discrepancy could have resulted from LC-MS detection bias or microbial conversion of the compounds into their more complex structural analogs (a hypothesis that requires further validation through targeted metabolomics).

As detailed in Table S8 and S9, expression levels of flavonoid compounds, such as kaempferol-3-O-rutinoside and epicatechin, increased during the first 4 days of fermentation. However, in the following 4 days, epicatechin, 5-O-caffeoylquinic acid, and other compounds showed an overall downward trend. Such changes aligned with the results obtained from the antioxidant activity assays. On the basis of the previous studies reporting that flavonoid content decreased after fermentation, flavonoid compounds could be continuously released from EUL residues during the early stages of fermentation but the rate at which microorganisms converted or degraded them exceeded the rate of release, leading to a decrease in content during later stages. Gallic acid and other phenolic compounds primarily upregulated after fermentation owing to microbial metabolism. Some relevant literatures indicated that plant polyphenols

primarily existed in the form of glycosides, which could be broken down by microorganisms into small-molecule polyphenols (Shabbir et al., 2021). The observed downregulation of certain glycosides, such as strychnine glycoside (Table S7), further supported the microbial decomposition of polyphenolic glycosides during fermentation.

Comprehensive analysis across different fermentation stages revealed that all three comparison groups involved multiple amino acid metabolic pathways and were enriched with related differential metabolites. Amino acids, such as *L*-glutamic acid, *L*-aspartic acid, and *L*-tryptophan, showed a decreasing trend during fermentation, indicating their utilization as precursors for the biosynthesis of other amino acid derivatives that demonstrated an increasing trend, such as phenylacetylglutamine and leucyl ketone. In addition to amino acid metabolism pathways, several conversion pathways between sugars and organic acids were highly significant ( $p < 0.01$ ) in the three groups, highly consistent with the metabolic activities of yeast and AAB in kombucha. In summary, postfermentation EUL kombucha accumulated substantial amounts of sugars, organic acids, and flavonoid-related metabolites, with its primary metabolic pathways being considerably associated with microbial growth and primary metabolism. The results were consistent with the findings reported in studies on TK (Li et al., 2025). Carbohydrates, amino acids, and organic acids were directly associated with the flavor of kombucha fermentation broth. Metabolites such as flavonoids and phenolic acids exhibited a certain connection with the physiological activities of kombucha fermentation broth (Xiao et al., 2021; Xiao et al., 2024). However, the specific metabolic pathways and mechanisms of key metabolites require further elucidation.

### 3.5. Analysis of microbial diversity in EUL kombucha

Alpha diversity analysis (Fig. 5A) assessed the richness and diversity among microbial communities using multiple indices and compared the differences in indices between different groups via intergroup difference tests (Müller & Nebel, 2021). Results indicated that the Shannon, ACE, Chao, and Sob index values initially increased followed by a decrease with fermentation time, whereas the Simpson index showed the opposite trend to that of the Shannon index, indicating that the diversity and abundance of bacterial communities increased during the early stages of fermentation but decreased during the middle and late stages. This decline in the later stages could be related to the prolonged fermentation time, causing a continuous decrease in pH, resulting in the inability of many acid-intolerant bacteria to survive. The sequencing coverage value of all the samples was as high as 99.99%, indicating sufficient sequencing depth and reliable results. To investigate differences in the bacterial community composition among samples with different fermentation days, PCoA was performed on the basis of the OTU level. Fig. 5B shows that the bacterial community composition of samples with the same fermentation time was highly similar, while samples with different fermentation times showed significant differences ( $p < 0.01$ ). The Venn diagram (Fig. 5C) showed that there were 13 shared bacterial OTUs throughout fermentation, while the number of unique OTUs increased from six initially to 23 on day 4 and then decreased to three on day 8.

The  $\alpha$ -diversity of the yeast community in EUL kombucha exhibited a distinct trend from that of bacteria (Fig. 6A). The Shannon, ACE, Chao, and Sob indices steadily increased over time, whereas the Simpson index declined, collectively indicating a progressive increase in both diversity and richness of the yeast community throughout fermentation. The sequencing coverage value was 99.99%, ensuring the reliability of the results. The PCoA based on the OTU level (Fig. 6B) revealed clear separation between groups, confirming significant differences in yeast community composition across fermentation times ( $p < 0.01$ ). The Venn diagram (Fig. 6C) showed that there were 13 OTUs; the number of unique OTUs increased from eight at the beginning to 13 on day 4 and then to 21 on day 8.

Statistical analysis of bacterial community structures across different

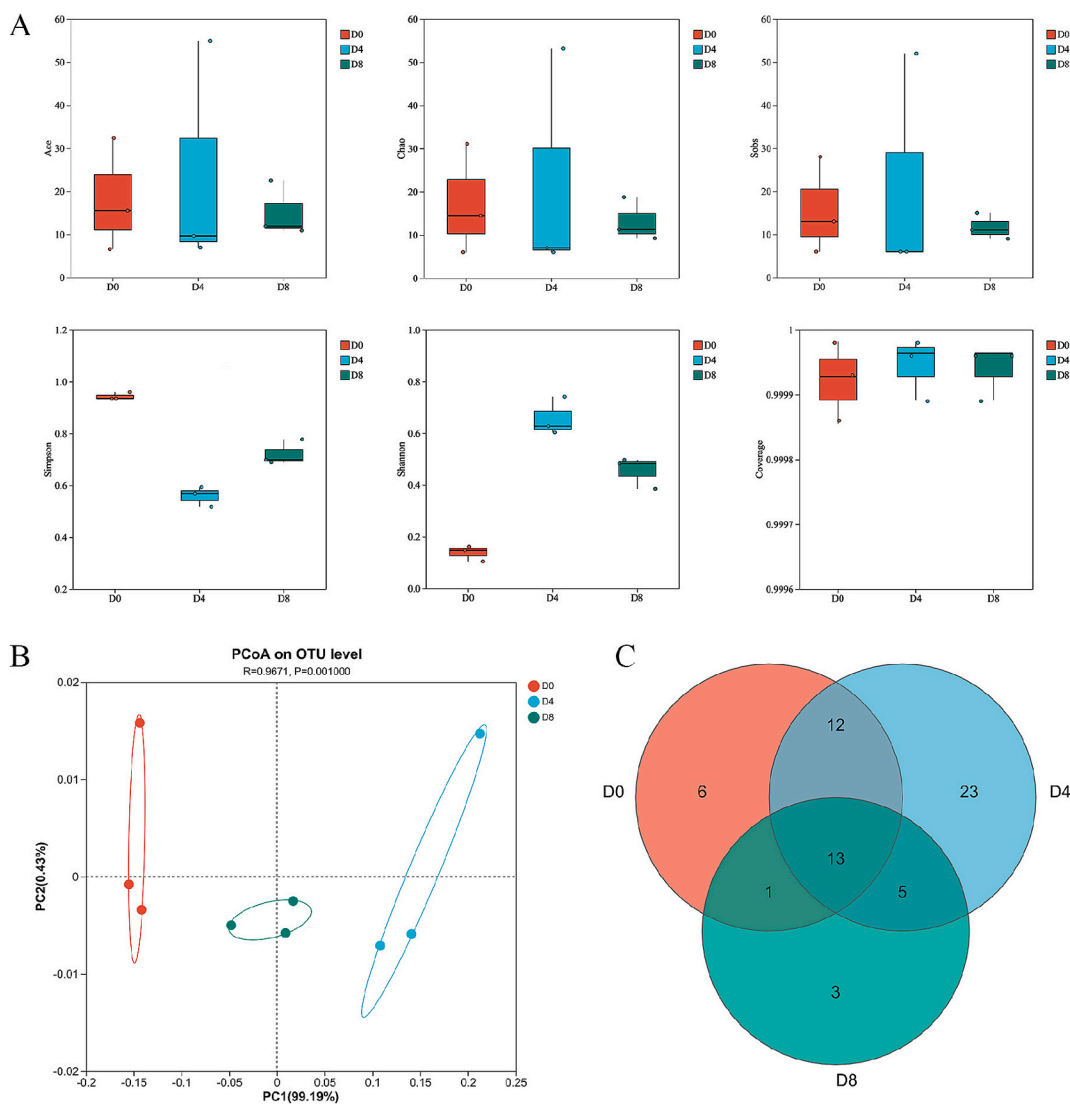


**Fig. 5.** Diversity and composition of bacterial communities during fermentation. (A) Box plots of  $\alpha$ -diversity indices (Ace, Chao, Sobs, Simpson, Shannon, and Coverage) across different fermentation days. (B) PCoA score plot based on OTU levels illustrating the  $\beta$ -diversity of bacterial communities. Ellipses denote clustering of bacterial communities at each fermentation day. (C) Venn diagram showing unique and shared OTUs. D0 is shown in red, D4 in blue, and D8 in green. Supplementary Table S10–13 provide relevant information. (For interpretation of the references to colour in this figure legend, the reader is referred to the web version of this article.)

fermentation days intuitively demonstrated the distribution characteristics of bacterial communities at the genus level during EUL kombucha fermentation. As shown in Fig. 7A, the main bacteria detected throughout the fermentation cycle were *Komagataeibacter*, *Gluconobacter*, and *Acetobacter*. *Komagataeibacter* and *Gluconobacter* were the dominant bacterial genera during fermentation, consistent with the findings of Barbosa et al. (2021). At D0, the relative abundance of *Komagataeibacter* reached its highest level (94.69%). As the fermentation period progressed, the relative abundance of *Komagataeibacter* first decreased (60.95%) and then increased (80.03%). Concurrently, the relative abundance of *Gluconobacter* showed a trend of first increasing (32.27%) and then decreasing (15.71%), while the relative abundance of *Acetobacter* during fermentation on D4 was 2.15%. During EUL kombucha fermentation, *Komagataeibacter* exhibited a competitive advantage and proliferated continuously as fermentation progressed, ultimately forming a stable microbial community structure that was conducive to fermentation together with *Gluconobacter* and *Acetobacter*. *Komagataeibacter* exhibited the unique ability to produce cellulose and organic acids, playing a key role in promoting sweet and sour characteristics, while *Acetobacter* participated in the formation of flavor

compounds such as gluconic acid and glucuronic acid (Subbiahdoss et al., 2022). However, unlike previous studies that reported the presence of *Lactobacillus* in kombucha, no *Lactobacillus* were found in samples that used EUL as the fermentation substrate (Meng et al., 2024). The absence of *Lactobacillus* could be attributed to the nutritional characteristics of the EUL fermentation substrate itself and kombucha starters obtained from different regions, which exhibited a certain degree of strain selectivity and are therefore were unsuitable for the growth of certain microorganisms (Peng et al., 2023).

Fig. 7B shows the yeast community structure at the genus level for EUL kombucha. The predominant yeasts detected throughout the fermentation cycle were *Dekkera*, *Hanseniaspora*, *Kregervanrija*, and *Zygosaccharomyces*. Of these, on D0, the relative abundance of *Hanseniaspora* and *Kregervanrija* was relatively high, at 53.15% and 45.10%, respectively. By the mid-fermentation and late fermentation stage, the relative abundances of *Hanseniaspora* and *Dekkera* were relatively high. The relative abundances of *Hanseniaspora* decreased from 80.38% to 56.52%, whereas those of *Dekkera* increased from 17.88% to 42.11%. *Hanseniaspora*, *Dekkera*, and *Kregervanrija* yeast genera dominated the EUL kombucha fermentation. At present, the types of yeast identified in

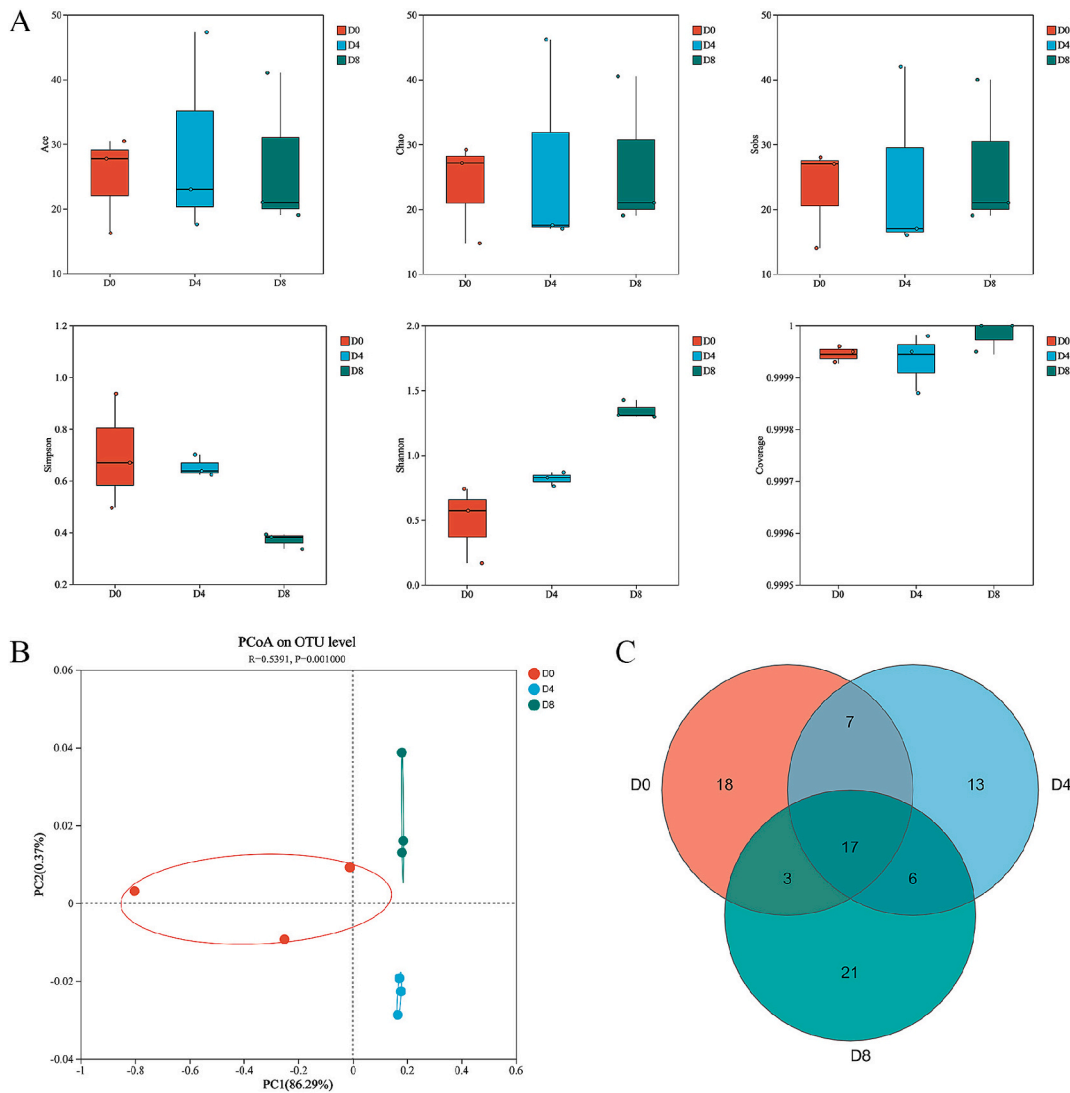


**Fig. 6.** Diversity and composition of yeast communities during fermentation. (A) Box plots of  $\alpha$ -diversity indices (Ace, Chao, Sobs, Simpson, Shannon, and Coverage) across different fermentation days. (B) PCoA score plot based on OTU levels illustrating the  $\beta$ -diversity of yeast communities. Ellipses indicate clustering of yeast communities at each fermentation day. (C) Venn diagram showing unique and shared OTUs. D0 is shown in red, D4 in blue, and D8 in green. Supplementary Table S14–17 provide the relevant information. (For interpretation of the references to colour in this figure legend, the reader is referred to the web version of this article.)

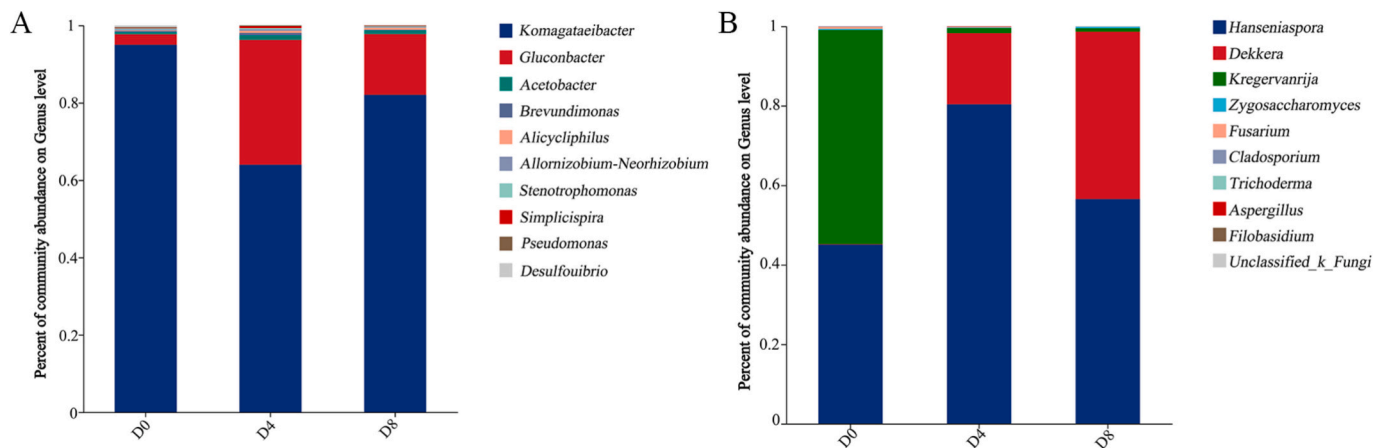


**Fig. 7.** Relative abundance of bacteria (A) and yeast (B) in EUL kombucha across different fermentation days. Representative sequence information is provided in Supplementary Table S13 and S17.

TK differed from those detected in EUL kombucha. This difference was associated with the source of the kombucha and the EUL substrate (Xiao et al., 2024). Microbial metabolic pathways could generally be divided into carbohydrate, protein, and lipid metabolism. The types of carbon sources, proteins, and fats available in tea leaves differed from those observed in EUL, and some microorganisms in kombucha were not suitable for growth in EUL kombucha (Zhou et al., 2022).

### 3.6. Spearman's correlation analysis

Spearman's correlation analysis was employed on physicochemical components, active components, metabolites, and microbial diversity of EUL kombucha on different fermentation days. Fig. 8A shows the correlation between the physicochemical components and dominant bacterial communities of EUL kombucha, while Fig. 8B shows the correlation between the bioactive compounds and in vitro antioxidant capacity of EUL kombucha and dominant bacterial communities. Among bacteria, *Komagataeibacter* was negatively associated with multiple antioxidant indicators and key bioactive compounds, such as succinic acid, total phenols, and RU but positively correlated with total flavonoids. By contrast, *Gluconobacter* exhibited an opposing correlation pattern with such components, suggesting a potential competitive relationship between these two bacteria in the fermentation system. *Acetobacter* showed a positive correlation with DPPH and IRP, likely

attributable to its acid-producing metabolism that enhanced polyphenol solubility and stability. Among yeasts, *Dekkera* demonstrated strong positive correlations with oxalic acid, malic acid, acetic acid, total phenols, and antioxidant activities, highlighting its central role in driving acidification and phenolic compound accumulation. Conversely, *Kregervanrija* was positively linked to CA content but negatively associated with total acids and phenols, indicating a potential inhibitory effect on overall fermentation progress and bioactive compound generation. In other words, dynamic changes in the microbial community led to changes in the fundamental characteristics of EUL kombucha.

These correlation data indicated that the EUL kombucha fermentation was a complex system driven by dynamic interactions between bacterial and yeast communities. *Komagataeibacter*, known for its role in cellulose synthesis, could contribute to biofilm formation by competing for carbon sources (e.g., glucose) during the mid- to late fermentation stages, thereby stabilizing the broth structure (Wang et al., 2022). Conversely, *Komagataeibacter* could reduce antioxidant activity by suppressing polyphenol oxidation or decomposing organic acids such as malic acid. By contrast, *Acetobacter*, which oxidizes ethanol to acetic acid, likely enhanced the solubility and activity of polyphenolic compounds (e.g., total phenols and RU) through acidification, consistent with studies showing improved stability and bioactivity of plant polyphenols in acidic environments (Keshk & Sameshima, 2005; Zubaidah et al., 2017). Similarly, *Gluconobacter* reinforced this acidic milieu by

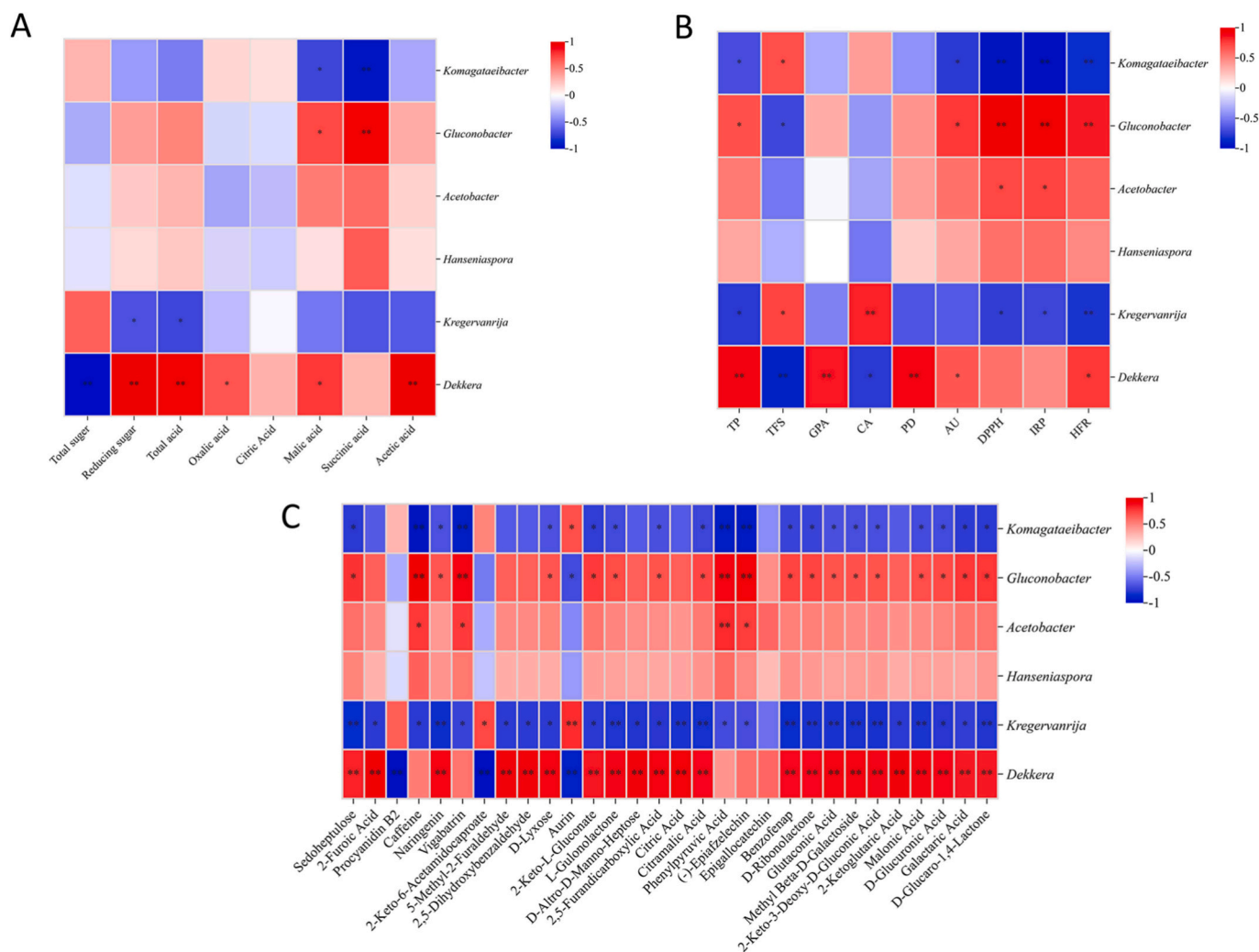


**Fig. 8.** Heat map showing correlations between physicochemical components (A), active components (B), differential metabolites (C), and core microbial communities of EUL kombucha. Spearman's correlation coefficients ranging from  $-1$  to  $+1$ . Red indicates a positive correlation ( $r > 0$ ), whereas blue indicates a negative correlation ( $r < 0$ ).  $**p < 0.05$ ,  $***p < 0.01$ . (For interpretation of the references to colour in this figure legend, the reader is referred to the web version of this article.)

producing gluconic acid, while glucose oxidation-derived gluconic acid lactone could further contribute to antioxidant capacity. Within this microbial network, the *Dekkera* functioned as a key glycolytic organism, generating ethanol and organic acids that in turn functioned as crucial substrates for AAB, illustrating a tightly coupled yeast–bacteria interaction that drove metabolic progress and functional properties of the fermentation system (Grassi et al., 2022).

The relationship between microbial communities and metabolite production during fermentation was extremely important for understanding the quality of kombucha (Yao et al., 2023). To investigate the influence of microbial communities on metabolites during the fermentation of EUL kombucha, the top 30 differentially abundant metabolites ( $VIP > 1$ ,  $p < 0.05$ ) from untargeted metabolomics and core bacterial genera in the fermentation broth were selected for correlation analysis (Fig. 8C). *Komagataeibacter* showed a highly significant negative correlation with caffeine, vigabatrin, phenylpyruvic acid, and epiafzelechin and showed significant negative correlations with sedoheptulose, naringin, D-lyxose, 2-keto-L-gluconate, L-gulonolactone, 2,5-furandicarboxylic, citramalic acid, benzofenap, D-ribonolactone, glutaconic acid, methyl-β-D-galactoside, 2-keto-3-deoxy-D-gluconic acid, malonic acid, D-glucuronic acid, galactaric acid, and D-gluconic-1,4-lactone. Furthermore, *Komagataeibacter* showed a significant positive correlation with aurin. *Komagataeibacter* and *Gluconobacter* behaved in opposite ways. *Acetobacter* showed a significant positive correlation with caffeine, vigabatrin, and epiafzelechin and a highly significant positive correlation with phenylpyruvic acid. *Dekkera* was highly significantly positively correlated with 22 fermentation metabolites, namely sedoheptulose, naringin, and D-glucono-1,4-lactone. *Dekkera* showed a highly significant negative correlation with procyanidin B2, 2-keto-6-acetamidocaproate, and aurin. *Kregervanrija* and *Dekkera* demonstrated almost opposite trends. Notably, *Kregervanrija* showed a significant negative correlation with phenylpyruvic acid and epiafzelechin, which were crucial for oxidizing the main catechins into theaflavins (Xiao et al., 2024). The results indicated that the secondary metabolites were influenced by the structural changes in the core microbial community, consistent with the findings of Wang et al. (2024). Specifically, *Komagataeibacter* and *Kregervanrija* showed a negative correlation with metabolites that were considerably upregulated during fermentation and exhibited a positive correlation with metabolites that were markedly downregulated. By contrast, *Gluconobacter* and *Dekkera* exhibited the opposite trend in their correlations with the relevant differentially expressed metabolites. Further analysis revealed that the metabolic pathways involved in such differential metabolites primarily included nucleotide metabolism, pentose and glucuronic acid-related conversions, ascorbic acid and aldehyde metabolism, and flavonoid biosynthesis. In other words, during of EUL kombucha fermentation, *Komagataeibacter*, *Gluconobacter*, and *Acetobacter*, together with *Dekkera* and *Kregervanrija*, could regulate metabolic pathways, thereby changing the expression of differential metabolites in the fermentation broth.

#### 4. Conclusion

This study demonstrated that EUL could be an alternative fermentation substrate for kombucha production. Changes in the microbial community structure played a crucial role in the conversion of components and were directly shaped by the quality of EUL kombucha during fermentation. In this process, *Komagataeibacter*, *Gluconobacter*, and *Acetobacter*, along with *Dekkera* and *Kregervanrija*, were identified as key drivers. Further studies should validate these results by systematically studying changes in microbial communities in kombucha made at different origins. In addition, future researchers should explore the specific mechanisms of action of the key microbial communities involved in the biotransformation of specific functional components, thereby clarifying their metabolic pathways and regulatory networks.

Supplementary data to this article can be found online at <https://doi.org/10.1016/j.foodchem.2026.148266>.

#### CRedit authorship contribution statement

**Lin Feng Wang:** Writing – original draft, Visualization, Software, Methodology, Formal analysis, Data curation, Conceptualization. **Erfeng Wang:** Writing – original draft, Visualization, Software, Methodology, Formal analysis, Data curation, Conceptualization. **Weipeng Wang:** Writing – original draft, Methodology, Data curation. **Wei Zhang:** Writing – original draft, Methodology, Data curation, Conceptualization. **Yifan Ge:** Writing – original draft, Methodology, Conceptualization. **Xiaokang Cao:** Writing – original draft, Methodology, Conceptualization. **Hong (Sabrina) Tian:** Writing – review & editing. **Xingke Li:** Writing – review & editing, Validation, Supervision, Methodology, Investigation, Funding acquisition, Formal analysis, Data curation, Conceptualization. **Xianfeng Zhu:** Writing – review & editing, Validation, Supervision, Methodology, Investigation, Formal analysis, Conceptualization.

#### Funding

This study was funded by grants from the Henan Provincial Key R&D Special Project (No. 241111110700).

#### Declaration of competing interest

The authors declare that they have no known competing financial interests or personal relationships that could have appeared to influence the work reported in this paper.

#### Acknowledgments

This study was supported by the Henan Provincial Key R&D Special Project (Grant No. 241111110700).

#### Data availability

Data will be made available on request.

#### References

- Anantachoke, N., Duangrat, R., Sutthiphakul, T., Ochaikul, D., & Mangmool, S. (2023). Kombucha beverages produced from fruits, vegetables, and plants: A review on their pharmacological activities and health benefits. *Foods (Basel, Switzerland)*, 12(9). Doi: 10.3390/foods12091818.
- Applegate, K. B., Cheek, P. R., & Inlow, J. K. (2019). Analysis of kombucha to teach biochemical concepts and techniques to undergraduate students. *Biochemistry and Molecular Biology Education*, 47(4), 459–467. <https://doi.org/10.1002/bmb.21240>
- Barbosa, C. D., Uetanabaro, A. P. T., Santos, W. C. R., Caetano, R. G., Albano, H., Kato, R., et al. (2021). Microbial-physicochemical integrated analysis of kombucha fermentation. *LWT- Food Science and Technology*, 148, Article 111788. <https://doi.org/10.1016/j.lwt.2021.111788>
- Cardoso, R. R., Neto, R. O., Dos Santos D'almeida, C. T., Do Nascimento, T. P., Pressete, C. G., Azevedo, L., et al. (2020). Kombuchas from green and black teas have different phenolic profile, which impacts their antioxidant capacities, antibacterial and antiproliferative activities. *Food Research International*, 128, Article 108782. <https://doi.org/10.1016/j.foodres.2019.108782>
- Chakravorty, S., Bhattacharya, S., Bhattacharya, D., Sarkar, S., & Gachhui, R. (2019). 10 - Kombucha: A promising functional beverage prepared from tea. In A. M. Grumezescu, & A. M. Holban (Eds.), *Non-alcoholic beverages* (pp. 285–327). Woodhead Publishing. <https://doi.org/10.1016/B978-0-12-815270-6.00010-4>.
- Chen, Q., Zhu, Y., Liu, Y., Liu, Y., Dong, C., Lin, Z., & Teng, J. (2022). Black tea aroma formation during the fermentation period. *Food Chemistry*, 374, Article 131640. <https://doi.org/10.1016/j.foodchem.2021.131640>
- Cheng, K. C., Wu, J. Y., Lin, J. T., & Liu, W. H. (2013). Enhancements of isoflavone aglycones, total phenolic content, and antioxidant activity of black soybean by solid-state fermentation with *Rhizopus* spp. *European Food Research and Technology*, 236(6), 1107–1113. <https://doi.org/10.1007/s00217-013-1936-7>
- Coton, M., Pawtowski, A., Taminiau, B., Burgaud, G., Deniel, F., et al. (2017). Unraveling microbial ecology of industrial-scale Kombucha fermentations by metabarcoding and culture-based methods. *FEMS Microbiology Ecology*, 93(5). <https://doi.org/10.1093/femsec/fix048>
- Dartora, B., Crepalde, L. T., Hickert, L. R., Fabricio, M. F., Ayub, M. A. Z., Veras, F. F., et al. (2023). Kombuchas from black tea, green tea, and yerba-mate decocts: Perceived sensory map, emotions, and physicochemical parameters. *International*

- Journal of Gastronomy and Food Science*, 33, Article 100789. <https://doi.org/10.1016/j.jgfs.2023.100789>
- De Filippis, F., Troise, A. D., Vitaglione, P., & Ercolini, D. (2018). Different temperatures select distinctive acetic acid bacteria species and promotes organic acids production during Kombucha tea fermentation. *Food Microbiology*, 73, 11–16. <https://doi.org/10.1016/j.fm.2018.01.008>
- Ding, Y. X., Dou, D. Q., Guo, Y. J., & Li, Q. (2014). Simultaneous quantification of eleven bioactive components of male flowers of *Eucommia ulmoides* oliver by HPLC and their quality evaluation by chemical fingerprint analysis with hierarchical clustering analysis. *Pharmacognosy Magazine*, 10(40), 435–440. <https://doi.org/10.4103/0973-1296.141813>
- Duan, Y., Guo, F., Li, C., Xiang, D., Gong, M., Yi, H., et al. (2024). Aqueous extract of fermented *Eucommia ulmoides* leaves alleviates hyperlipidemia by maintaining gut homeostasis and modulating metabolism in high-fat diet fed rats. *Phytomedicine*, 128, Article 155291. <https://doi.org/10.1016/j.phymed.2023.155291>
- Emiljanowicz, K. E., & Malinowska-Pańczyk, E. (2020). Kombucha from alternative raw materials - the review. *Critical Reviews in Food Science and Nutrition*, 60(19), 3185–3194. <https://doi.org/10.1080/10408398.2019.1679714>
- Esatbeyoglu, T., Sarikaya Aydin, S., Gültekin Subasi, B., Erskine, E., Gök, R., Ibrahim, S. A., et al. (2024). Additional advances related to the health benefits associated with kombucha consumption. *Critical Reviews in Food Science and Nutrition*, 64(18), 6102–6119. <https://doi.org/10.1080/10408398.2022.2163373>
- Ferreira, A. M., & Mendes-Faia, A. (2020). The role of yeasts and lactic acid Bacteria on the metabolism of organic acids during winemaking. *Foods (Basel, Switzerland)*, 9(9). <https://doi.org/10.3390/foods9091231>
- Ford, E. S., & Choi, H. K. (2013). Associations between concentrations of uric acid with concentrations of vitamin a and beta-carotene among adults in the United States. *Nutrition research (New York, N.Y.)*, 33(12), 995–1002. <https://doi.org/10.1016/j.nutres.2013.08.008>
- Freitas, A., Sousa, P., & Wurlitzer, N. (2022). Alternative raw materials in kombucha production. *International Journal of Gastronomy and Food Science*, 30, Article 100594. <https://doi.org/10.1016/j.ijgfs.2022.100594>
- Grassi, A., Cristani, C., Palla, M., Giorgi, R. D., Giovannetti, M., & Agnolucci, M. (2022). Storage time and temperature affect microbial dynamics of yeasts and acetic acid bacteria in a kombucha beverage. *International Journal of Food Microbiology*, 382, Article 109934. <https://doi.org/10.1016/j.ijfoodmicro.2022.109934>
- Healy, L., Zhu, X., Dong, G., Selli, S., Kelebek, H., Sullivan, C., et al. (2024). Investigation into the use of novel pretreatments in the fermentation of *Alaria esculenta* by *Lactiplantibacillus plantarum* and kombucha SCOBY. *Food Chemistry*, 442, Article 138335. <https://doi.org/10.1016/j.foodchem.2023.138335>
- Huang, H., Han, M. H., Gu, Q., Wang, J. D., Zhao, H., Zhai, B. W., et al. (2023). Identification of pancreatic lipase inhibitors from *Eucommia ulmoides* tea by affinity-ultrafiltration combined UPLC-Orbitrap MS and *in vitro* validation. *Food Chemistry*, 426, Article 136630. <https://doi.org/10.1016/j.foodchem.2023.136630>
- Hur, S. J., Lee, S. Y., Kim, Y. C., Choi, I., & Kim, G. B. (2014). Effect of fermentation on the antioxidant activity in plant-based foods. *Food Chemistry*, 160, 346–356. <https://doi.org/10.1016/j.foodchem.2014.03.112>
- Jakubczyk, K., Kaldunska, J., Kochman, J., & Janda, K. (2020). Chemical profile and antioxidant activity of the Kombucha beverage derived from white, green. *Antioxidants (Basel)*, 9(5), 447. <https://doi.org/10.3390/antiox9050447>
- Jakubczyk, K., Łopusiewicz, Ł., Kika, J., Janda-Milczarek, K., & Skonieczna-Zydecka, K. (2024). Fermented tea as a food with functional value—Its microbiological profile, antioxidant potential and phytochemical composition. *Foods*, 13(1), 50. <https://www.mdpi.com/2304-8158/13/1/50>
- Jayabalan, R., Malbasa, R. V., Loncar, E. S., Vitas, J. S., & Sathishkumar, M. (2014). A review on kombucha tea microbiology, composition, fermentation, beneficial effects, toxicity, and tea fungus. *Comprehensive Reviews in Food Science and Food Safety*, 13(4), 538–550. <https://doi.org/10.1111/1541-4337.12073>
- Jayabalan, R., Malbasa, R. V., & Sathishkumar, M. (2017). Kombucha tea: metabolites. In *Fungal metabolites* (pp. 1–14). [https://doi.org/10.1007/978-3-319-19456-1\\_12-1](https://doi.org/10.1007/978-3-319-19456-1_12-1)
- Jayabalan, R., Malini, K., Sathishkumar, M., Swaminathan, K., & Yun, S. E. (2010). Biochemical characteristics of tea fungus produced during Kombucha fermentation. *Food Science and Biotechnology*, 19(3), 843–847. <https://doi.org/10.1007/s10068-010-0119-6>
- Jayabalan, R., Marimuthu, S., & Swaminathan, K. (2007). Changes in content of organic acids and tea polyphenols during kombucha tea fermentation. *Food Chemistry*, 102(1), 392–398. <https://doi.org/10.1016/j.foodchem.2006.05.032>
- Júnior, J. C. D. S., Mafaldo, Í. M., Brito, I. D. L., & Cordeiro, A. M. T. D. M. (2022). Kombucha: Formulation, chemical composition, and therapeutic potentialities. *Current Research in Food Science*, 5, 360–365. <https://doi.org/10.1016/j.crf.2022.01.023>
- Keshk, S., & Sameshima, K. (2005). Evaluation of different carbon sources for bacterial cellulose production. *African Journal of Biotechnology*, 4(6), 478–482. <https://doi.org/10.5897/AJB2005.000-3087>
- Kitwetchareon, H., Phung, L. T., Klanrit, P., Thanonkeo, S., Tippayawat, P., Yamada, M., & Thanonkeo, P. (2023). Kombucha healthy drink-recent advances in production, chemical composition and health benefits. *Fermentation-Basel*, 9(1), Article 48. <https://doi.org/10.3390/fermentation9010048>
- Klopotek, Y., Otto, K., & Böhm, V. (2005). Processing strawberries to different products alters contents of vitamin C, total phenolics, total anthocyanins, and antioxidant capacity. *Journal of Agricultural and Food Chemistry*, 53(14), 5640–5646. <https://doi.org/10.1021/jf047947v>
- Lambros, M., Tran, T. H., Fei, Q., & Nicolaou, M. (2022). Citric acid: A multifunctional pharmaceutical excipient. *Pharmaceutics*, 14(5), 972. <https://doi.org/10.3390/pharmaceutics14050972>
- Leali, N. F., Binati, R. L., Martelli, F., Gatto, V., Luzzini, G., Salini, A., et al. (2022). Reconstruction of simplified microbial consortia to modulate sensory quality of Kombucha tea. *Foods (Basel, Switzerland)*, 11(19). <https://doi.org/10.3390/foods11193045>
- Li, S., Bi, P., Sun, N., Gao, Z., Chen, X., & Guo, J. (2022). Characterization of different non-Saccharomyces yeasts via mono-fermentation to produce polyphenol-enriched and fragrant kiwi wine. *Food Microbiology*, 103, Article 103867. <https://doi.org/10.1016/j.fm.2021.103867>
- Li, S., Wang, S., Wang, L., Liu, X., Wang, X., Cai, R., et al. (2023). Unraveling symbiotic microbial communities, metabolomics and volatilomics profiles of kombucha from diverse regions in China. *Food Research International*, 174, Article 113652. <https://doi.org/10.1016/j.foodres.2023.113652>
- Li, S. Q., Chen, X. W., Gao, Z. Y., Zhang, Z., Bi, P. F., & Guo, J. (2023). Enhancing antioxidant activity and fragrant profile of low-ethanol kiwi wine via sequential culture of indigenous *Zygosaccharomyces rouxii* and *Saccharomyces cerevisiae*. *Food Bioscience*, 51, Article 102210. <https://doi.org/10.1016/j.fbio.2022.102210>
- Li, X., Tso, N., Huang, S., Wang, J., Zhou, Y., & Liu, R. (2025). A comprehensive evaluation of microbial synergistic metabolic mechanisms and health benefits in Kombucha fermentation: A review. *Biology*, 14(8), 952. <https://doi.org/10.3390/biology14080952>
- Li, X. Y., Fu, Y. J., Fu, Y. F., Wei, W., Xu, C., Yuan, X. H., & Gu, C. B. (2022). Simultaneous quantification of fourteen characteristic active compounds in *Eucommia ulmoides* Oliver and its tea product by ultra-high performance liquid chromatography coupled with triple quadrupole mass spectrometry (UPLC-QqQ-MS/MS). *Food Chemistry*, 389, Article 133106. <https://doi.org/10.1016/j.foodchem.2022.133106>
- Liao, R., Xia, Q., Zhou, C., Geng, F., Wang, Y., Sun, Y., et al. (2022). LC-MS/MS-based metabolomics and sensory evaluation characterize metabolites and texture of normal and spoiled dry-cured hams. *Food Chemistry*, 371, Article 131156. <https://doi.org/10.1016/j.foodchem.2021.131156>
- Liu, M., Zhang, L., Li, J., Xu, G., Zong, W., & Wang, L. (2024). Effects of lactic acid bacteria on antioxidant activity *in vitro* and aroma component of *Eucommia ulmoides* tea. *Journal of Food Science and Technology*, 61(1), 169–177. <https://doi.org/10.1007/s13197-023-05833-w>
- Liu, X., & Locasale, J. W. (2017). Metabolomics: A primer. *Trends in Biochemical Sciences*, 42(4), 274–284. <https://doi.org/10.1016/j.tibs.2017.01.004>
- Mao, X., Yue, S.-J., Xu, D.-Q., Fu, R.-J., Han, J.-Z., Zhou, H.-M., & Tang, Y.-P. (2023). Research progress on flavor and quality of Chinese Rice wine in the brewing process. *ACS Omega*, 8(36), 32311–32330. <https://doi.org/10.1021/acsoomega.3c04732>
- Martínez Leal, J., Valenzuela Suárez, L., Jayabalan, R., Huerta Oros, J., & Escalante-Aburto, A. (2018). A review on health benefits of kombucha nutritional compounds and metabolites. *CyTA Journal of Food*, 16(1), 390–399. <https://doi.org/10.1080/19476337.2017.1410499>
- May, A., Narayanan, S., Alcock, J., Varsani, A., Maley, C., & Aktipis, A. (2019). Kombucha: A novel model system for cooperation and conflict in a complex multi-species microbial ecosystem. *PeerJ*, 7, Article e7565. <https://doi.org/10.7717/peerj.7565>
- Meng, Y., Wang, X., Li, Y., Chen, J., & Chen, X. (2024). Microbial interactions and dynamic changes of volatile flavor compounds during the fermentation of traditional kombucha. *Food Chemistry*, 430, Article 137060. <https://doi.org/10.1016/j.foodchem.2023.137060>
- Mohd Ariff, R., Chai, X. Y., Chang, L. S., Fazry, S., Othman, B. A., & Lim, S. J. (2023). Recent trends in Kombucha: Conventional and alternative fermentation in development of novel beverage. *Food Bioscience*, 53, Article 102714. <https://doi.org/10.1016/j.fbio.2023.102714>
- Muhalidin, B. J., Osman, F. A., Muhamad, R., Sapawi, C., Anzian, A., Voon, W. W. Y., & Hussin, A. S. M. (2019). Effects of sugar sources and fermentation time on the properties of tea fungus (kombucha) beverage. *International Food Research Journal*, 26(2), 481–487. <https://doi.org/10.1016/j.ifrj.2019.01.018>
- Müller, R., & Nebel, M. (2021). On the use of sequence-quality information in OTU clustering. *PeerJ*, 9, Article 11717. <https://doi.org/10.7717/peerj.11717>
- Özyurt, H. (2020). Changes in the content of total polyphenols and the antioxidant activity of different beverages obtained by Kombucha ‘tea fungus’. *International Journal of Agriculture Environment and Food Sciences*, 4(3), 255–261. <https://doi.org/10.31015/JAEFS.2020.3.3>
- Peng, X. H., Yue, Q., Chi, Q. Q., Liu, Y. W., Tian, T., Dai, S. C., et al. (2023). Microbial diversity and flavor regularity of soy milk fermented using kombucha. *Foods*, 12(4), Article 884. <https://doi.org/10.3390/foods12040884>
- Procházková, D., Bousová, I., & Wilhelmová, N. (2011). Antioxidant and prooxidant properties of flavonoids. *Fitoterapia*, 82(4), 513–523. <https://doi.org/10.1016/j.fitote.2011.01.018>
- Selvaraj, S., & Gurusurthy, K. (2024). Metagenomic, organoleptic profiling, and nutritional properties of fermented kombucha tea substituted with recycled substrates. *Frontiers in Microbiology*, 15, Article 1367697. <https://doi.org/10.3389/fmicb.2024.1367697>
- Shabbir, U., Rubab, M., Daliri, E. B. M., Chelliah, R., Javed, A., & Oh, D. H. (2021). Curcumin, quercetin, catechins and metabolic diseases: The role of gut microbiota. *Nutrients*, 13(1), 206. <https://doi.org/10.3390/nu13010206>
- Shi, X., Luo, S., Zhong, K., Hu, X., & Zhang, Z. (2022). Chemical profiling, quantitation, and bioactivities of Du-Zhong tea. *Food Chemistry*, 394, Article 133552. <https://doi.org/10.1016/j.foodchem.2022.133552>
- Subbiahdoss, G., Osmen, S., & Reimhult, E. (2022). Cellulosic biofilm formation of *Komagataeibacter* in kombucha at oil-water interfaces. *Biofilm*, 4, Article 100071. <https://doi.org/10.1016/j.biofilm.2022.100071>
- Sun, T. Y., Li, J. S., & Chen, C. (2015). Effects of blending wheatgrass juice on enhancing phenolic compounds and antioxidant activities of traditional kombucha beverage.

- Journal of Food and Drug Analysis*, 23(4), 709–718. <https://doi.org/10.1016/j.jfda.2015.01.009>
- Tefon-Öztürk, B. E., Eroglu, B., Delik, E., Çiçek, M., & Çiçek, E. (2023). Comprehensive evaluation of three important herbs for Kombucha fermentation. *Food Technology and Biotechnology*, 61(1), 127–137. <https://doi.org/10.17113/ftb.61.01.23.7789>
- Thaipong, K., Boonprakob, U., Crosby, K., Cisneros-Zevallos, L., & Byrne, D. H. (2006). Comparison of ABTS, DPPH, FRAP, and ORAC assays for estimating antioxidant activity from guava fruit extracts. *Journal of Food Composition and Analysis*, 19(6–7), 669–675. <https://doi.org/10.1016/j.jfca.2006.01.003>
- Tu, C., Yu, T., Feng, S., Xu, N., Massawe, A., Shui, S., & Zhang, B. (2024). Dynamics of microbial communities, flavor, and physicochemical properties of kombucha-fermented *Sargassum fusiforme* beverage during fermentation [article]. *LWT- Food Science and Technology*, 192, Article 115729. <https://doi.org/10.1016/j.lwt.2024.115729>
- Villarreal-Soto, S. A., Beaufort, S., Bouajila, J., Souchard, J. P., Renard, T., Ronan, S., & Taillandier, P. (2019). Impact of fermentation conditions on the production of bioactive compounds with anticancer, anti-inflammatory and antioxidant properties in kombucha tea extracts. *Process Biochemistry*, 83, 44–54. <https://doi.org/10.1016/j.procbio.2019.05.004>
- Wang, X., Wang, D., Wang, H., Jiao, S., Wu, J., Hou, Y., et al. (2022). Chemical profile and antioxidant capacity of Kombucha tea by the pure cultured Kombucha. *LWT- Food Science and Technology*, 168, Article 113931. <https://doi.org/10.1016/j.lwt.2022.113931>
- Wang, Z., Peng, S., Peng, M., She, Z., Yang, Q., & Huang, T. (2020). Adsorption and desorption characteristics of polyphenols from *Eucommia ulmoides* Oliv. Leaves with macroporous resin and its inhibitory effect on  $\alpha$ -amylase and  $\alpha$ -glucosidase. *Annals of translational medicine*, 8(16), 1004. <https://doi.org/10.21037/atm-20-5468>
- Wang, Z. Q., Li, H. Y., Huang, W. M., Duan, S. Q., Yan, Y., Zeng, Z., et al. (2024). Landscapes of the main components, metabolic and microbial signatures, and their correlations during pile-fermentation of Tibetan tea. *Food Chemistry*, 430, Article 136932. <https://doi.org/10.1016/j.foodchem.2023.136932>
- Watawana, M. I., Jayawardena, N., Gunawardhana, C. B., & Waisundara, V. Y. (2015). Health, wellness, and safety aspects of the consumption of kombucha. *Journal of Chemistry*, , Article 591869. <https://doi.org/10.1155/2015/591869>
- Xiao, Y., Chen, H., Chen, Y., Ho, C.-T., Wang, Y., Cai, T., et al. (2024). Effect of inoculation with different *Eurotium cristatum* strains on the microbial communities and volatile organic compounds of Fu brick tea. *Food research international (Ottawa, Ont.)*, 197(Pt 1), Article 115219. <https://doi.org/10.1016/j.foodres.2024.115219>
- Xiao, Y., Wu, X., Yao, X., Chen, Y., Ho, C.-T., He, C., et al. (2021). Metabolite profiling, antioxidant and  $\alpha$ -glucosidase inhibitory activities of buckwheat processed by solid-state fermentation with *Eurotium cristatum* YL-1. *Food research international (Ottawa, Ont.)*, 143, Article 110262. <https://doi.org/10.1016/j.foodres.2021.110262>
- Xiong, R. G., Wu, S. X., Cheng, J., Saimaiti, A., Liu, Q., et al. (2023). Antioxidant activities, phenolic compounds, and sensory acceptability of kombucha-fermented beverages from bamboo leaf and mulberry leaf. *Antioxidants*, 12(8), Article 1573. <https://doi.org/10.3390/antiox12081573>
- Xu, C., Yu, Z., Zhou, S., Feng, H., Du, Q., et al. (2025). Dynamic changes in physicochemical, bacterial, and volatile profiles during kombucha fermentation of mulberry fruits and leaves. *Food research international (Ottawa, Ont.)*, 218, Article 116813. <https://doi.org/10.1016/j.foodres.2025.116813>
- Xu, J., Hou, H., Hu, J., & Liu, B. (2018). Optimized microwave extraction, characterization and antioxidant capacity of biological polysaccharides from *Eucommia ulmoides* Oliver leaf. *Scientific Reports*, 8(1), 6561. <https://doi.org/10.1038/s41598-018-24957-0>
- Xu, X., Miao, Y., Wang, H., Ye, P., Li, T., Li, C., & et al. (2022). A snapshot of microbial succession and volatile compound dynamics in flat peach wine during spontaneous fermentation. *Frontiers in Microbiology*, 13, Article 919047. <https://doi.org/10.3389/fmicb.2022.919047>
- Xu, Y., Yao, L., Song, S., Sun, M., Wang, H., Yu, C., et al. (2024). Revealing the microbial diversity and volatile flavor formation in finger citron kombucha by metagenomic and GC-MS analysis. *Food Bioscience*, 59, Article 104087. <https://doi.org/10.1016/j.fbio.2024.104087>
- Yang, J., Zhang, Z. Z., Wu, Q. M., Ding, X. Y., Yin, C. Y., Yang, E. D., et al. (2022). Multiple responses optimization of antioxidative components extracted from fenugreek seeds using response surface methodology to identify their chemical compositions. *Food Science & Nutrition*, 10(10), 3475–3484. <https://doi.org/10.1002/fsn3.2949>
- Yao, L. Y., Zhang, J., Lu, J., Chen, D., Song, S. Q., Wang, H. T., et al. (2023). Revealing the influence of microbiota on the flavor of kombucha during natural fermentation process by metagenomic and GC-MS analysis. *Food Research International*, 169, Article 112909. <https://doi.org/10.1016/j.foodres.2023.112909>
- Yuan, T.-Y., Fang, L.-H., Lv, Y., & Du, G.-H. (2013). Advance in study on pharmacological effect of *Eucommia folium*. *Zhongguo Zhong yao za zhi = Zhongguo zhongyao zazhi = China journal of Chinese materia medica*, 38(6), 781–785. <https://www.ncbi.nlm.nih.gov/pubmed/23717951>
- Zeng, X., Wang, Y., Jia, H., Wang, Z., Gao, Z., Luo, Y., et al. (2022). Metagenomic analysis of microflora structure and functional capacity in probiotic Tibetan kefir grains. *Food Research International*, 151, Article 110849. <https://doi.org/10.1016/j.foodres.2021.110849>
- Zhang, C., Zheng, X., Ma, C., & Qiao, Q. (2020). Determination of organic acids, alcohols and glucose content in barley wine by HPLC. *Food Science and Technology*, 45(07), 317–323. <https://doi.org/10.13684/j.cnki.spkj.2020.07.054>
- Zheng, Y., Liu, Y., Han, S., He, Y., Liu, R., & Zhou, P. (2024). Comprehensive evaluation of quality and bioactivity of kombucha from six major tea types in China. *International Journal of Gastronomy and Food Science*, 36, Article 100910. <https://doi.org/10.1016/j.ijgfs.2024.100910>
- Zhou, D. D., Saimaiti, A., Luo, M., Huang, S. Y., Xiong, R. G., Shang, A., et al. (2022). Fermentation with tea residues enhances antioxidant activities and polyphenol contents in kombucha beverages. *Antioxidants*, 11(1), Article 155. <https://doi.org/10.3390/antiox11010155>
- Zubaidah, E., Yurista, S., Rahmadani, N. R., & Iop. (2017). Characteristic of physical, chemical, and microbiological kombucha from various varieties of apples. *IOP Conference Series: Earth and Environmental Science*, 131, Article 012040. <https://doi.org/10.1088/1755-1315/131/1/012040> (International conference on green agro-industry and bioeconomy (icgab 2017)).